energies

Article

Evaluation of Ride Performance of Active Inerter-Based Vehicle Suspension System with Parameter Uncertainties and Input Constraint via Robust H_∞ Control

Keyvan Karim Afshar *, Roman Korzeniowski and Jarosław Konieczny *

Department of Process Control, AGH University of Science and Technology, Al. Mickiewicza 30, 30-059 Krakow, Poland
* Correspondence: afshar@agh.edu.pl (K.K.A.); koniejar@agh.edu.pl (J.K.)

Abstract: In this study, we investigate a robust H_∞ controller for a quarter-car model of an active inerter-based suspension system under parameter uncertainties and road disturbance. Its main objective is to improve the inherent compromises between ride quality, handling performance, suspension stroke, and energy consumption. Inerters have been extensively used to suppress unwanted vibrations from various kinds of mechanical structures. The advantage of inerter is that the realized ratio of equivalent mass (inertance relative to the mass of the primary structure) is greater than its actual mass ratio, resulting in higher performance for the same effective mass. First, the dynamics and state space of the active inerter-based suspension system were achieved for the quarter-car model with parameter uncertainties. In order to attain the defined objectives, and ensure that the closed-loop system achieves the prescribed disturbance attenuation level, the Lyapunov stability function, and linear matrix inequality (LMI) techniques have been utilized to satisfy the robust H_∞ criterion. Furthermore, to limit the gain of the controller, some LMIs have been added. In the case of feasibility, sufficient LMI conditions by solving a convex optimization problem afford the stabilizing gain of the robust state-feedback controller. According to numerical simulations, the active inerter-based suspension system in the presence of parameter uncertainties and external disturbance performs much better than both a passive suspension with inerter and active suspension without inerter.

Keywords: robust H_∞ control; active inerter-based suspension system; quarter-car model; linear matrix inequality

check for updates

Citation: Karim Afshar, K.; Korzeniowski, R.; Konieczny, J. Evaluation of Ride Performance of Active Inerter-Based Vehicle Suspension System with Parameter Uncertainties and Input Constraint via Robust H_∞ Control. *Energies* **2023**, *16*, 4099. https://doi.org/10.3390/en16104099

Academic Editor: Oscar Barambones

Received: 21 March 2023
Revised: 11 May 2023
Accepted: 12 May 2023
Published: 15 May 2023

1. Introduction

The main objective in the development of vehicle suspension systems is not only to reduce the acceleration of the vehicle's body and its passengers but also to preserve good tire-road contact. The suspension travel must also be restricted within the permitted working space [1]. These purposes (ride comfort, suspension stroke, and road holding) can conflict with each other, thus the design problem is to find a compromise between them [1,2]. There are three major categories of the control structure for suspension systems that have been developed to acquire the desired performance of the vehicle: passive, semi-active, and active suspension systems [1]. Numerous investigations have demonstrated that the active suspension system is a useful method for enhancing the suspension performance [3]. Nowadays, research to improve suspension performance is mostly concerned with two areas: first, the exact and logical design of advanced vehicle suspension, and second, the look for the best control strategies.

In order to mitigate the effects of vibration, numerous methods have been developed, including isolating systems from vibration, controlling systems, redesigning systems to adjust their natural frequencies, employing tuning mass dampers/absorbers, and more [4,5]. Tuned mass dampers (TMDs) are widely employed to suppress unwanted vibrations of various mechanical structures, e.g., buildings, bridges, motorcycle steering systems, vehicle and train suspensions, landing gear suspensions, etc. [4,5]. The classical TMD is a mass on a linear spring, and it is well-known that the classical TMD is particularly efficient at reducing the response of the main structure in principal resonance, but at other frequencies (even ones that are close to the resonance frequency) it enhances the system's motion amplitude [4,5]. Therefore, we must always consider whether we want to most effectively damp vibrations at a particular frequency or whether we want to achieve tolerable damping characteristics over a wide range of vibration frequencies. This problem is capable to be minimized by novel TMDs containing inerters or magnetorheological dampers, which are increasingly being developed nowadays [6]. An inerter is a device with two free-moving terminals whose generated force is proportional to the relative acceleration of its terminals. The proportional constant is called inertance with the unit kilogram [7]. The inerter possesses the effect of mass amplification and would provide much greater inertia compared to its own mass, thus increasing the inertia of the entire dynamic system rather than increasing the mass [5,7]. Because of its mechanical properties, it is therefore an efficient structure for damping vibrations. On the other hand, the primary driving reason for the proposal of inerter lies in the fact that the force-current analogy between mechanical and electrical systems is not complete. Introducing the inerter has completed the analogy between the mechanical network spring-damper-inerter and the electrical network inductor-resistor-capacitor. As a result, the systematic approaches for the synthesis of electrical networks can be employed for the development of inerter-based mechanical networks directly [4].

The rack-and-pinion, ball-screw, and hydraulic (or fluid) inerters are the three most commonly used inerters. Depending on whether a flywheel is used in the realization, they can be divided into two categories, namely flywheel-based inerters and non-flywheel inerters. When the inertance is fixed, the inerter is passive; when the inertance can be adjusted, the inerter is semi-active [4,6].

The inerter is employed as a passive element in the majority of applications, in the sense that online control activities cannot adjust the inertance. Then the performance of the system has been evaluated passively or actively using the controller [4]. In [8], analytical solutions for some inerter-based suspension structures were established for a quarter-car model, and the performance advantages of utilizing inerters in vehicle suspensions were analytically presented. In [9], several performance requirements for passive suspensions with inerters, including ride comfort, suspension stroke, and tire deflection, were analytically studied. Consequently, the analytical solutions for six suspension configurations were taken, revealing that the performance indices of complex networks are superior to those of simpler networks. In [10], the nonlinearities of inerter and their influence on suspension performance have been investigated. A mechatronic network structure that combines a permanent magnet electric machine and a ball-screw inerter was suggested in [11]. One of the main advantages of this mechatronic structure is the ability to combine mechanical and electrical networks to actualize the system impedance. As a result, it is simple and takes up little space to realize the higher-order system impedance. In [12], eight inerter-based networks have been combined with sky-hook controlled and ground-hook controlled actuators to demonstrate the performance advantages of inerter. In [13], the active inerter-based suspension has employed a controllable actuator to generate the required force. Although it uses the most energy, it offers higher dynamic performance as compared to passive and semi-active suspensions.

Active suspensions provide the best performance but require more energy due to the force-generating actuators. To solve this problem, an inerter-based electromagnetic device was presented in [14] and implemented in the vehicle suspension system. The proposed device not only improves the performance of the suspension, but also generates an amount of electrical energy that can be used by other parts of the vehicle, especially the energy required to operate the actuator.

To find a compromise between the conflicting performances of the vehicle suspension system, many approaches have been proposed based on various control techniques, such as sliding mode control [15,16], fuzzy logic and neural network control [1,17], model predictive control [18], adaptive control [15,17], H_∞ control [2,19–21], etc. In particular, the application of robust H_∞ control of the active vehicle suspension system in the context of robustness and damping of road disturbances has been intensively investigated. Additionally, it has been recognized that it is not only an effective way to trade-off between conflicting performance requirements, but also to optimize either a weighted single objective function with hard constraints or a multi-objective function [1,19].

The majority of problems that engineers face in practical applications contain some degree of uncertainty, including model and parameter uncertainties. Accordingly, while developing a control system for stability and performance, system uncertainties should always be taken into account [22]. Changes in the inertial properties of the vehicle, such as vehicle's sprung mass (due to the number of passengers in the vehicle, the load it is carrying, or the aerodynamic forces), have a direct impact on the ride comfort, handling, and braking performance of the vehicle. Additionally, uncertainty with regard to stiffness may be caused by a variety of factors, including variability in manufacturing processes and quality control, uncertainty in material properties and element dimensions, etc. It can be challenging to select a fixed inerter that will satisfy vehicle performance requirements at the sprung mass natural frequency without considerably deteriorating at the unsprung mass natural frequency [23]. Therefore, when evaluating the performance of the inerter-based vehicle suspension system, uncertainty in the inertance of inerter should be taken into account.

To resolve the problems mentioned earlier, a parameter-dependent control approach could be devoted to realizing robust control of vehicle suspension systems independent of changes in vehicle parameters. The linear matrix inequality (LMI) approach is a practical and effective method for handling system uncertainties [22]. In [20], a robust sampled-data control for uncertain active vehicle suspension systems with input time-delay was presented. In [24], by employing a quadratic Lyapunov function, adequate conditions for a state feedback-based H_∞ controller and an observer-based H_∞ controller were presented in the form of non-convex matrix inequalities that take actuator saturation into account. In [2], a delay-dependent memory state-feedback H_∞ controller for active quarter-car suspension system with input time-delay in the presence of external disturbance were investigated. In [21], for a class of nonlinear systems under parametric uncertainties and external disturbances, a nonlinear state feedback controller based on linear matrix inequality was presented. Considering all these works, we intend to investigate the active inerter-based suspension system for a quarter-car model by considering all factors, including external disturbance, parametric uncertainty, and input constraint. It is worth noting that this work is not a simple application of an existing method on active suspension systems, but that the theoretical findings are also novel and nontrivial.

In this paper, the active inerter-based quarter-car suspension system is investigated based on the parallel-connected configuration, since this configuration is simple and space-saving [7]. The H_∞ control (energy-to-energy) is used to optimize the performance requirements of the active inerter-based suspension system in the presence of parameter uncertainties and external disturbance. Employing the direct Lyapunov method, sufficient stability requirements and performance criteria are taken in the form of LMIs. Moreover, to reduce the controller gain, additional LMIs are also added to the original condition, which results in avoiding the amplification of the measurement noise and saturation of the actuator [3].

The main contributions of this work can be summarized as follows:

- In this paper, we purpose to design a multi-objective robust H_∞ controller for the active inerter-based quarter-car suspension system that provides a compromise between the basic performance requirements for vehicle suspension system including ride comfort, suspension deflection, road holding, and energy consumption.

- We have presented the state space of the active vehicle suspension system for the quarter-car model with the presence of inerter in its dynamics and evaluate the performance of this system using the robust H_∞ controller.
- In the actual implementation of the active suspension system, a high gain controller might cause major problems including noise amplification and actuator saturation. In order to prevent such problems, some additional LMIs are introduced to reduce the gain of the controller.
- The stability conditions are derived as linear matrix inequalities (LMIs) and therefore the stabilization gain of the system is obtained by solving the convex optimization problem.

The subsequent parts of this paper are structured into four sections. The description of the active inerter-based quarter-car suspension system is provided in Section 2. The problem formulation for robust H_∞ control based on the solvability of LMIs for the uncertain system is given in Section 3. In Section 4, the proposed controller is applied to the inerter-based quarter-car model for performance evaluation. Finally, the conclusion of our findings is presented in Section 5.

Notation: The following nomenclature will be utilized throughout this paper. In a symmetric block matrix or complex matrix expressions, an asterisk $(*)$ indicates a term that is induced by symmetry. The notation $\mathbf{P} > 0$ (≥ 0) is utilized to denote that $\mathbf{P}$ is a real symmetric and positive definite (semi-definite) matrix. R^n stands for the n-dimensional Euclidean space and the superscript T denotes matrix transposition. $\mathbf{I}$ and $\mathbf{0}$ are utilized to indicate the identity and zero matrices with appropriate dimensions, and $diag\{\cdots\}$ stands for a block-diagonal matrix. Let $\|\bullet\|$ symbolize the induced norm for matrices and the Euclidean norm for vectors. $\|\bullet\|_{\mathcal{L}_2}$ represents the $\mathcal{L}_2$ norm of a signal defined as $\|\mathbf{v}(t)\|_{\mathcal{L}_2}^2 = \int_0^\infty \|\mathbf{v}(s)\|^2 ds$.

2. Active Inerter-Based Quarter-Car Suspension System Modelling

Since the force generated by the spring relies on the displacement, and the force produced by the damper depends on the velocity, the idea of the inerter is to act against accelerations. Accordingly, the inerter is connected in parallel to the spring and damper between the wheel and the chassis. The main function of the inerter is to dampen the vibrations coming from the tire, which enhance the contact between the wheel and the ground [23]. The quarter-car model of the active suspension system equipped with inerter, as shown in Figure 1, can be reduced to 2DOF system considering the vertical dynamics. The model is assembled by one sprung mass (car body) that is connected to one unsprung mass. The unsprung masses is free to move vertically and are confronted with the road disturbance input.

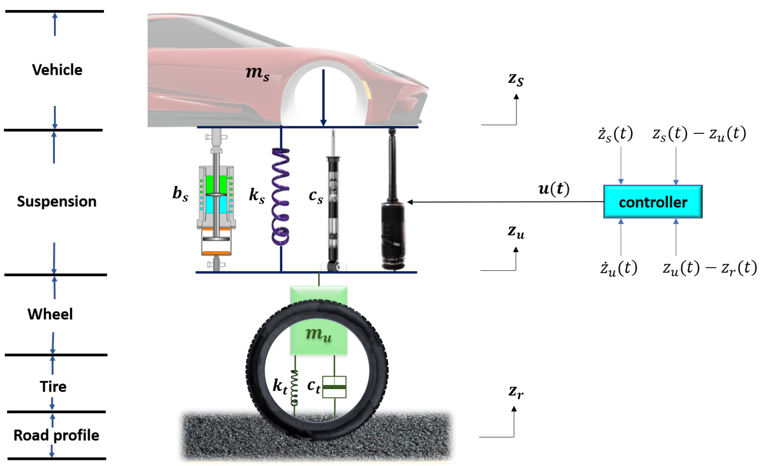

Figure 1. Quarter-car model of active Inerter-based suspension system.

In Figure 1, m_s represents the mass of the car body, and m_u is the unsprung mass. b_s denotes the inertance of the inerter, c_s represents the damping coefficient of suspension element, and k_s represents the stiffness of the suspension. Likewise, k_t is the tire stiffness, and c_t is damping of the pneumatic tire; $u(t)$ denotes actuator force input. $z_s(t)$ represents the vertical displacements of the body, $z_u(t)$ denotes the vertical displacements of the unsprung mass, and $z_r(t)$ denotes the road disturbance input. It is assumed that the tire is always in contact with the ground, and the characteristics of the suspension elements are linear.

We assume that the exact value of the sprung mass $m_s(t)$ and inertance of the inerter $b_s(t)$ are not known, but their maximum and minimum values are available. The differential equations of motion can be calculated with the help of Newton's second law as follows

$$m_s(t)\ddot{z}_s(t) + b_s(t)[\ddot{z}_s(t) - \ddot{z}_u(t)] + c_s[\dot{z}_s(t) - \dot{z}_u(t)] + k_s[z_s(t) - z_u(t)] = u(t) \tag{1}$$

$$\begin{aligned} &m_u\ddot{z}_u(t) + b_s(t)[\ddot{z}_u(t) - \ddot{z}_s(t)] + c_s[\dot{z}_u(t) - \dot{z}_s(t)] + k_s[z_u(t) - z_s(t)] \\ &+c_t[\dot{z}_u(t) - \dot{z}_r(t)] + k_t[z_u(t) - z_r(t)] = -u(t) \end{aligned} \tag{2}$$

It is noteworthy that the equations of motion for the passive suspension system can be received by letting $u(t) = 0$. Defining four state variables as follow

$$\begin{aligned} x_1(t) &= z_s(t) - z_u(t) \quad , \quad x_2(t) = z_u(t) - z_r(t) \\ x_3(t) &= \dot{z}_s(t) \quad\quad\quad\;\; , \quad x_4(t) = \dot{z}_u(t) \end{aligned} \tag{3}$$

where $x_1(t)$ represents the suspension deflection, $x_2(t)$ is the tire deflection, $x_3(t)$ denotes the vertical velocity of the car body, $x_4(t)$ represents the vertical velocity of the wheel. Accordingly, by defining $\mathbf{x}(t) = \begin{bmatrix} x_1(t) & x_2(t) & x_3(t) & x_4(t) \end{bmatrix}^T$, the active inerter-based suspension system can be represented by the following state-space equation

$$\dot{\mathbf{x}}(t) = \mathbf{A}(t)\mathbf{x}(t) + \mathbf{B}(t)\mathbf{u}(t) + \mathbf{D}(t)\mathbf{v}(t) \tag{4}$$

where

$$\mathbf{A}(t) = \begin{bmatrix} 0 & 0 & 1 & -1 \\ 0 & 0 & 0 & 1 \\ -m_u k_s/f(t) & -b_s(t)k_t/f(t) & -m_u c_s/f(t) & (m_u c_s - b_s(t)c_t)/f(t) \\ m_s(t)k_s/f(t) & -(m_s(t)+b_s(t))k_t/f(t) & m_s(t)c_s/f(t) & -(m_s(t)c_s + (m_s(t)+b_s(t))c_t)/f(t) \end{bmatrix}$$

$$\mathbf{B}(t) = \begin{bmatrix} 0 & 0 & m_u/f(t) & -m_s(t)/f(t) \end{bmatrix}^T$$

$$\mathbf{D}(t) = \begin{bmatrix} 0 & -1 & b_s(t)c_t/f(t) & (m_s(t)+b_s(t))c_t/f(t) \end{bmatrix}^T$$

$$\begin{aligned} f(t) &= m_s(t)m_u + (m_s(t)+m_u)b_s(t) \\ \mathbf{v}(t) &= \dot{z}_r(t) \end{aligned}$$

As mentioned earlier, ride comfort, suspension deflection, and road-holding ability are the three most important performance criteria to consider when developing controllers for vehicle suspension systems.

- **Ride comfort:** Indeed, minimization of the vertical acceleration sensed by the rider is the paramount assignment of the suspension system, leading to ride comfort and less depreciation. In other words, ride comfort is the general sensation of noise, vibration and motion inside a driven vehicle and it impacts the comfort, safety and health of the passengers. Therefore, the sprung mass acceleration $\ddot{z}_s(t)$ is selected as the first control output vector.
- **Suspension deflection limitation:** Vehicle suspension must be capable of support the vehicle's static weight. Accordingly, in order to prevent mechanical structural damage and ride comfort deterioration, the active suspension controllers should be qualified to preclude the suspension from hitting its travel limit.
- **Road holding ability:** In practical vehicle systems, during maneuvers such as deaccelerating, accelerating, or cornering, there are numerous forces acting on the

wheel that can raise it off the ground and leads to losing control of the car, in either steering senses or driving. Hence, the dynamic tire load should not exceed the static tire load to guarantee firm uninterrupted contact of the wheel to the road [2].

Therefore, the controlled output of the active inerter-based suspension system can be presented by the following state space equation:

$$\mathbf{z}(t) = \mathbf{C}_1(t)\,\mathbf{x}(t) + \mathbf{D}_{12}(t)\,\mathbf{u}(t) + \mathbf{F}(t)\,\mathbf{v}(t) \tag{5}$$

where

$$\mathbf{C}_1(t) = \begin{bmatrix} -\rho(m_u k_s/f(t)) & -\rho(b_s(t)k_t/f(t)) & -\rho(m_u c_s/f(t)) & \rho((m_u c_s - b_s(t)c_t)/f(t)) \\ \alpha & 0 & 0 & 0 \\ 0 & \beta & 0 & 0 \end{bmatrix}$$

$$\mathbf{D}_{12}(t) = \begin{bmatrix} \rho(m_u/f(t)) \\ 0 \\ 0 \end{bmatrix} \quad , \quad \mathbf{F}(t) = \begin{bmatrix} \rho(b_s(t)c_t/f(t)) \\ 0 \\ 0 \end{bmatrix}$$

where $\rho > 0$ is a scalar weighting for the ride comfort, $\alpha > 0$ is a scalar weighting for the suspension deflection, and $\beta > 0$ is a scalar weighting for the tire deflection. They have been utilized to manage the compromise between control objectives [2].

It is worth noting that with the new sensor configuration for intelligent vehicles, vehicle states such as vertical speed and attitude can be accurately estimated. Some of these states are important inputs for vehicle suspension system control [25]. We suppose the case that all the state variables $\mathbf{x}(t)$ can be measured, leading to the design of a state-feedback H_∞ controller.

$$\mathbf{y}(t) = \mathbf{C}_2\,\mathbf{x}(t) \quad , \mathbf{C}_2 = \mathbf{I} \tag{6}$$

For the design of the robust H_∞ controller, the following state-feedback controller is considered

$$\mathbf{u}(t) = \mathbf{K}\mathbf{y}(t) = \mathbf{K}\mathbf{x}(t) \tag{7}$$

where $\mathbf{K}$ is the state-feedback gain matrix that must be designed in such a way that, first, the closed-loop system in the absence of external disturbance is asymptotically stable, and second, under zero initial conditions the $\mathcal{L}_2$ gain (i.e., H_∞ norm) of the closed-loop system guarantees $\|\mathbf{z}(t)\|^2_{\mathcal{L}_2} < \gamma^2\|\mathbf{v}(t)\|^2_{\mathcal{L}_2}$ for all nonzero $\mathbf{v}(t) \in \mathcal{L}_2[\ 0 \quad \infty\ )$, and some scalar $\gamma > 0$.

3. Robust H_∞ Controller Design

The active inerter-based suspension system can be defined by the following state-space equations

$$\begin{aligned} \dot{\mathbf{x}}(t) &= \mathbf{A}(t)\mathbf{x}(t) + \mathbf{B}(t)\mathbf{u}(t) + \mathbf{D}(t)\mathbf{v}(t) \\ \mathbf{z}(t) &= \mathbf{C}_1(t)\mathbf{x}(t) + \mathbf{D}_{12}(t)\mathbf{u}(t) + \mathbf{F}(t)\mathbf{v}(t) \\ \mathbf{y}(t) &= \mathbf{C}_2\mathbf{x}(t) \\ \mathbf{x}(t) &= \phi(t) \end{aligned} \tag{8}$$

where $\mathbf{x}(t) \in R^n$ is the state, $\mathbf{u}(t) \in R^m$ is the input vector, $\mathbf{y}(t) \in R^p$ is the measured output, $\mathbf{z}(t) \in R^d$ is the controlled output, $\phi(t)$ is a real-valued initial function, $\mathbf{v}(t) \in R^q$ denotes the external disturbance vector, matrices $\mathbf{A}(t), \mathbf{B}(t), \mathbf{D}(t), \mathbf{C}_1(t), \mathbf{D}_{12}(t)$, and $\mathbf{F}(t)$, are all uncertain matrices with appropriate dimensions.

Define $\mho = \{\mathbf{A}(t), \mathbf{B}(t), \mathbf{D}(t), \mathbf{C}_1(t), \mathbf{D}_{12}(t), \mathbf{F}(t)\}$. Then for $\mathbf{\Theta}(t) \in \mho$ we have

$$\mathbf{\Theta}(t) = \mathbf{\Theta} + \Delta\mathbf{\Theta}(t) \tag{9}$$

where $\Delta\mathbf{\Theta}(t)$ represents the uncertainties. In addition, the uncertainties are assumed to be structurally bounded, i.e.,

$$\Delta\mathbf{\Theta}(t) = \mathbf{M}_\Theta\mathbf{E}(t)\mathbf{N}_\Theta \tag{10}$$

where $\mathbf{E}(t)^T\mathbf{E}(t) \leq \mathbf{I}$; moreover, $\mathbf{M}_\Theta$ and $\mathbf{N}_\Theta$ are appropriately dimensioned matrices.

In this section, we will solve the problem of the robust state-feedback H_∞ controller for active inerter-based suspension systems with parameter uncertainties and external disturbance. The equivalent structure for this controller is shown in Figure 2. Theorem 1 presents the conditions that without external disturbance, the uncertain closed-loop system becomes asymptotically stable, and in the presence of external disturbance, the desired amount of disturbance attenuation is reached. This can be accomplished by minimizing the H_∞ norm of the closed-loop system under the external disturbance $\mathbf{v}(t)$ to the controlled outputs $\mathbf{z}(t)$ via a suitable quadratic Lyapunov function.

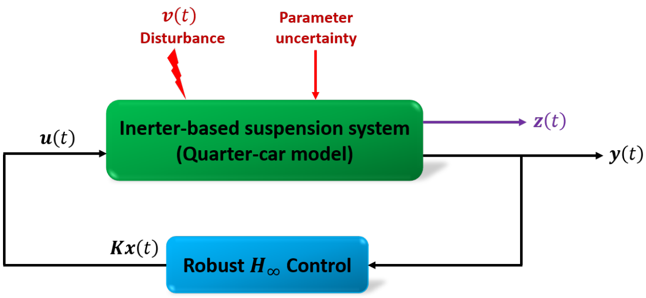

Figure 2. Equivalent structure of the robust H_∞ controller with parameter uncertainty and external disturbance.

Assumption 1. *In this paper, the external disturbance signal $\mathbf{v}(t)$ is considered to be square-integrable, that is*

$$\|\mathbf{v}(t)\|^2_{\mathcal{L}_2} = \int_0^\infty \|\mathbf{v}(s)\|^2 ds < v_{max} < \infty$$

Lemma 1 ([26])**.** *Let $\mathbf{Q}$, $\mathbf{\Phi}$ and $\mathbf{w}$ be real matrices of appropriate dimensions with $\mathbf{w}$ satisfying $\mathbf{w}^T\mathbf{w} \leq \mathbf{I}$. Then, for any scalar $\varepsilon > 0$*

$$\mathbf{Q}\mathbf{w}\mathbf{\Phi} + (\mathbf{Q}\mathbf{w}\mathbf{\Phi})^T \leq \varepsilon^{-1}\mathbf{Q}^T\mathbf{Q} + \varepsilon\,\mathbf{\Phi}^T\mathbf{\Phi} \tag{11}$$

Lemma 2 (Schur Complement [27])**.** *Given constant matrices $\mathbf{\Omega}_1$, $\mathbf{\Omega}_2$ and $\mathbf{\Omega}_3$ satisfying $\mathbf{\Omega}_1 = \mathbf{\Omega}_1^T$ and $\mathbf{\Omega}_2 > \mathbf{0}$, then $\mathbf{\Omega}_1 + \mathbf{\Omega}_3^T\mathbf{\Omega}_2^{-1}\mathbf{\Omega}_3 < \mathbf{0}$, if and only if*

$$\begin{bmatrix} \mathbf{\Omega}_1 & \mathbf{\Omega}_3^T \\ \mathbf{\Omega}_3 & -\mathbf{\Omega}_2 \end{bmatrix} < \mathbf{0} \tag{12}$$

Theorem 1. *Supposing positive constants γ, δ_1, L_R, and L_S, the linear uncertain active inerter-based suspension system (Equation (8)) with state-feedback controller in Equation (7) is asymptotically stable without external disturbance, and in the presence of external disturbance fulfills $\|\mathbf{z}(t)\|^2_{\mathcal{L}_2} < \gamma^2\|\mathbf{v}(t)\|^2_{\mathcal{L}_2}$ for $\mathbf{v}(t) \in \mathcal{L}_2[\,0 \quad \infty\,)$, if there exist symmetric positive definite matrix $\mathbf{X} > 0$, matrix $\mathbf{Y}$ with appropriate dimensions, and $\varepsilon_i > 0$ for $i = 1, \ldots, 9$, such that the following LMIs hold*

$$\begin{bmatrix} \bar{\mathbf{\Xi}} & \mathbf{\Psi} \\ * & \mathbf{\Gamma} \end{bmatrix} < 0 \tag{13}$$

$$\begin{bmatrix} L_R\mathbf{I} & \mathbf{Y}^T \\ \mathbf{Y} & \mathbf{I} \end{bmatrix} > 0 \tag{14}$$

$$\begin{bmatrix} L_S\mathbf{I} & \mathbf{I} \\ \mathbf{I} & \mathbf{X} \end{bmatrix} > 0 \tag{15}$$

where

$$\bar{\Xi} = \begin{bmatrix} \bar{\Xi}_{11} & \mathbf{D} & \mathbf{X}\mathbf{C_1}^T + \mathbf{Y}^T\mathbf{D_{12}}^T & \mathbf{0} & \mathbf{X}\mathbf{C_1}^T + \mathbf{Y}^T\mathbf{D_{12}}^T & \mathbf{0} \\ * & -\gamma^2\mathbf{I} & \mathbf{0} & \mathbf{F}^T & \mathbf{0} & \mathbf{F}^T \\ * & * & \bar{\Xi}_{33} & \mathbf{0} & \mathbf{0} & \mathbf{0} \\ * & * & * & \bar{\Xi}_{44} & \mathbf{0} & \mathbf{0} \\ * & * & * & * & \bar{\Xi}_{55} & \mathbf{0} \\ * & * & * & * & * & \bar{\Xi}_{66} \end{bmatrix}$$

$$\begin{aligned} \bar{\Xi}_{11} &= \mathbf{AX} + \mathbf{XA}^T + \mathbf{Y}^T\mathbf{B}^T + \mathbf{BY} + \varepsilon_1\mathbf{M}_A\mathbf{M}_A^T + \varepsilon_2\mathbf{M}_B\mathbf{M}_B^T + \varepsilon_3\mathbf{M}_D\mathbf{M}_D^T \\ \bar{\Xi}_{33} &= -\mathbf{I} + \varepsilon_4\mathbf{M}_{c_1}\mathbf{M}_{c_1}^T + \varepsilon_5\mathbf{M}_{D_{12}}\mathbf{M}_{D_{12}}^T \\ \bar{\Xi}_{44} &= -\delta_1\mathbf{I} + \varepsilon_6\mathbf{M}_F\mathbf{M}_F^T \\ \bar{\Xi}_{55} &= -\delta_1^{-1}\mathbf{I} + \varepsilon_7\mathbf{M}_{c_1}\mathbf{M}_{c_1}^T + \varepsilon_8\mathbf{M}_{D_{12}}\mathbf{M}_{D_{12}}^T \\ \bar{\Xi}_{66} &= -\mathbf{I} + \varepsilon_9\mathbf{M}_F\mathbf{M}_F^T \end{aligned}$$

$$\mathbf{\Psi} = \begin{bmatrix} \mathbf{XN}_A^T & \mathbf{Y}^T\mathbf{N}_B^T & \mathbf{0} & \mathbf{XN}_{c_1}^T & \mathbf{Y}^T\mathbf{N}_{D_{12}}^T & \mathbf{0} & \mathbf{XN}_{c_1}^T & \mathbf{Y}^T\mathbf{N}_{D_{12}}^T & \mathbf{0} \\ \mathbf{0} & \mathbf{0} & \mathbf{N}_D^T & \mathbf{0} & \mathbf{0} & \mathbf{N}_F^T & \mathbf{0} & \mathbf{0} & \mathbf{N}_F^T \\ \mathbf{0} & \mathbf{0} & \mathbf{0} & \mathbf{0} & \mathbf{0} & \mathbf{0} & \mathbf{0} & \mathbf{0} & \mathbf{0} \\ \mathbf{0} & \mathbf{0} & \mathbf{0} & \mathbf{0} & \mathbf{0} & \mathbf{0} & \mathbf{0} & \mathbf{0} & \mathbf{0} \\ \mathbf{0} & \mathbf{0} & \mathbf{0} & \mathbf{0} & \mathbf{0} & \mathbf{0} & \mathbf{0} & \mathbf{0} & \mathbf{0} \\ \mathbf{0} & \mathbf{0} & \mathbf{0} & \mathbf{0} & \mathbf{0} & \mathbf{0} & \mathbf{0} & \mathbf{0} & \mathbf{0} \end{bmatrix}$$

$$\mathbf{\Gamma} = diag(-\varepsilon_1\mathbf{I}, -\varepsilon_2\mathbf{I}, -\varepsilon_3\mathbf{I}, -\varepsilon_4\mathbf{I}, -\varepsilon_5\mathbf{I}, -\varepsilon_6\mathbf{I}, -\varepsilon_7\mathbf{I}, -\varepsilon_8\mathbf{I}, -\varepsilon_9\mathbf{I})$$

In this case, if inequalities Equations (13)–(15) have a feasible solution, the stabilizing gain of the state-feedback controller (Equation (7)) is given by $\mathbf{K} = \mathbf{YX}^{-1}$.

Proof. The Lyapunov function is chosen as follows:

$$V(t) = \mathbf{x}^T(t)\,\mathbf{p}\,\mathbf{x}(t) > 0 \tag{16}$$

and $\mathbf{p} = \mathbf{p}^T > 0$ is the matrix to be chosen. The derivative of $V(t)$ is taken as

$$\begin{aligned} \dot{V}(t) &= \dot{\mathbf{x}}^T(t)\,\mathbf{p}\,\mathbf{x}(t) + \mathbf{x}^T(t)\,\mathbf{p}\,\dot{\mathbf{x}}(t) \\ &= \mathbf{x}^T(t)(\mathbf{A}(t) + \mathbf{B}(t)\mathbf{K})^T\mathbf{p}\,\mathbf{x}(t) + \mathbf{v}^T(t)\mathbf{D}(t)^T\mathbf{p}\,\mathbf{x}(t) \\ &\quad + \mathbf{x}^T(t)\,\mathbf{p}(\mathbf{A}(t) + \mathbf{B}(t)\mathbf{K})\mathbf{x}(t) + \mathbf{x}^T(t)\,\mathbf{p}\,\mathbf{D}(t)\mathbf{v}(t) < 0 \end{aligned} \tag{17}$$

Supposing zero initial condition ($\mathbf{x}(t) = \phi(t) = 0$), we have $V(t)|_{t=0} = 0$. Now, we can suppose the following index

$$J_\infty = \int_0^\infty \left[\mathbf{z}_1(t)^T\mathbf{z}_1(t) - \gamma^2\mathbf{v}(t)^T\mathbf{v}(t)\right]dt \tag{18}$$

Then, for any nonzero $\mathbf{v}(t) \in \mathcal{L}_2[\,0 \quad \infty\,)$, there holds,

$$\begin{aligned} J_\infty &\le \int_0^\infty \left[\mathbf{z}_1(t)^T\mathbf{z}_1(t) - \gamma^2\mathbf{v}(t)^T\mathbf{v}(t)\right]dt + V(t)|_{t=\infty} - V(t)|_{t=0} \\ &= \int_0^\infty \left[\mathbf{z}_1(t)^T\mathbf{z}_1(t) - \gamma^2\mathbf{v}(t)^T\mathbf{v}(t) + \dot{V}(t)\right]dt = \int_0^\infty \zeta^T\mathbf{\Pi}_1\zeta\,dt \end{aligned} \tag{19}$$

It is supposed that $\zeta = \begin{bmatrix} \mathbf{x}(t)^T & \mathbf{v}(t)^T \end{bmatrix}^T$, and

$$\mathbf{\Pi}_1 = \begin{bmatrix} \mathbf{\Gamma}_{11} & (\mathbf{C}_1(t) + \mathbf{D}_{12}(t)\mathbf{K})^T\mathbf{F}(t) + \mathbf{p}\,\mathbf{D}(t)^T \\ * & \mathbf{F}(t)^T\mathbf{F}(t) - \gamma^2\mathbf{I} \end{bmatrix} \tag{20}$$

where

$$\mathbf{\Gamma}_{11} = (\mathbf{A}(t) + \mathbf{B}(t)\mathbf{K})^T\mathbf{p} + \mathbf{p}(\mathbf{A}(t) + \mathbf{B}(t)\mathbf{K}) + (\mathbf{C}_1(t) + \mathbf{D}_{12}(t)\mathbf{K})^T(\mathbf{C}_1(t) + \mathbf{D}_{12}(t)\mathbf{K})$$

Considering the zero-disturbance input ($\mathbf{v}(t) = 0$); if Equation (20) is negative-definite ($\mathbf{\Pi}_1 < 0$), then it can be concluded that $\dot{V}(t) < 0$ and the asymptotic stability of the system in Equation (8) is fulfilled. When $\mathbf{v}(t) \in \mathcal{L}_2[\,0 \quad \infty\,)$, and $\mathbf{\Pi}_1 < 0$, this indicates that $J_\infty < 0$ and therefore $\|\mathbf{z}(t)\|_{\mathcal{L}_2}^2 < \gamma^2\|\mathbf{v}(t)\|_{\mathcal{L}_2}^2$.

$\mathbf{\Pi}_1 < 0$ can be written as follows

$$\mathbf{\Pi}_1 = \begin{bmatrix} (\mathbf{A}(t)+\mathbf{B}(t)\mathbf{K})^T\mathbf{p}+\mathbf{p}(\mathbf{A}(t)+\mathbf{B}(t)\mathbf{K}) & (\mathbf{C}_1(t)+\mathbf{D}_{12}(t)\mathbf{K})^T\mathbf{F}(t)+\mathbf{p}\,\mathbf{D}(t) \\ * & \mathbf{F}(t)^T\mathbf{F}(t)-\gamma^2\mathbf{I} \end{bmatrix} + \begin{bmatrix} (\mathbf{C}_1(t)+\mathbf{D}_{12}(t)\mathbf{K})^T \\ \mathbf{0} \end{bmatrix}\mathbf{I}\begin{bmatrix} (\mathbf{C}_1(t)+\mathbf{D}_{12}(t)\mathbf{K}) & \mathbf{0} \end{bmatrix} < 0 \quad (21)$$

By utilizing Lemma 2 (Schur complement), $\mathbf{\Pi}_1 < 0$ is equivalent to

$$\mathbf{\Pi}_2 = \begin{bmatrix} (\mathbf{A}(t)+\mathbf{B}(t)\mathbf{K})^T\mathbf{p}+\mathbf{p}(\mathbf{A}(t)+\mathbf{B}(t)\mathbf{K}) & (\mathbf{C}_1(t)+\mathbf{D}_{12}(t)\mathbf{K})^T\mathbf{F}(t)+\mathbf{p}\,\mathbf{D}(t) & (\mathbf{C}_1(t)+\mathbf{D}_{12}(t)\mathbf{K})^T \\ * & \mathbf{F}(t)^T\mathbf{F}(t)-\gamma^2\mathbf{I} & \mathbf{0} \\ * & * & -\mathbf{I} \end{bmatrix} < 0 \quad (22)$$

As a result of Lemma 1, we can write the upper bound for $\mathbf{\Pi}_2$ in Equation (22) as follows

$$\begin{aligned} \mathbf{\Pi}_2 = {} & \begin{bmatrix} (\mathbf{A}(t)+\mathbf{B}(t)\mathbf{K})^T\mathbf{p}+\mathbf{p}(\mathbf{A}(t)+\mathbf{B}(t)\mathbf{K}) & \mathbf{p}\,\mathbf{D}(t) & (\mathbf{C}_1(t)+\mathbf{D}_{12}(t)\mathbf{K})^T \\ * & \mathbf{F}(t)^T\mathbf{F}(t)-\gamma^2\mathbf{I} & \mathbf{0} \\ * & * & -\mathbf{I} \end{bmatrix} \\ & + \begin{bmatrix} (\mathbf{C}_1(t)+\mathbf{D}_{12}(t)\mathbf{K})^T \\ \mathbf{0} \\ \mathbf{0} \end{bmatrix} I \begin{bmatrix} \mathbf{0} & \mathbf{F}(t) & \mathbf{0} \end{bmatrix} + \begin{bmatrix} \mathbf{0} \\ \mathbf{F}(t)^T \\ \mathbf{0} \end{bmatrix} I \begin{bmatrix} (\mathbf{C}_1(t)+\mathbf{D}_{12}(t)\mathbf{K}) & \mathbf{0} & \mathbf{0} \end{bmatrix} \\ \leq {} & \begin{bmatrix} (\mathbf{A}(t)+\mathbf{B}(t)\mathbf{K})^T\mathbf{p}+\mathbf{p}(\mathbf{A}(t)+\mathbf{B}(t)\mathbf{K}) & \mathbf{p}\,\mathbf{D}(t) & (\mathbf{C}_1(t)+\mathbf{D}_{12}(t)\mathbf{K})^T \\ * & \mathbf{F}(t)^T\mathbf{F}(t)-\gamma^2\mathbf{I} & \mathbf{0} \\ * & * & -\mathbf{I} \end{bmatrix} \\ & + \begin{bmatrix} \mathbf{0} \\ \mathbf{F}(t)^T \\ \mathbf{0} \end{bmatrix} \delta_1^{-1} \begin{bmatrix} \mathbf{0} & \mathbf{F}(t) & \mathbf{0} \end{bmatrix} + \begin{bmatrix} (\mathbf{C}_1(t)+\mathbf{D}_{12}(t)\mathbf{K})^T \\ \mathbf{0} \\ \mathbf{0} \end{bmatrix} \delta_1 \begin{bmatrix} (\mathbf{C}_1(t)+\mathbf{D}_{12}(t)\mathbf{K}) & \mathbf{0} & \mathbf{0} \end{bmatrix} \end{aligned} \quad (23)$$

Applying Schur complement to Equation (23), we get

$$\mathbf{\Pi}_3 = \begin{bmatrix} \hat{\mathbf{\Pi}}_{11} & \mathbf{p}\,\mathbf{D}(t) & \hat{\mathbf{\Pi}}_{13} & \mathbf{0} & \hat{\mathbf{\Pi}}_{15} \\ * & \mathbf{F}(t)^T\mathbf{F}(t)-\gamma^2\mathbf{I} & 0 & \mathbf{F}(t)^T & \mathbf{0} \\ * & * & -\mathbf{I} & \mathbf{0} & \mathbf{0} \\ * & * & * & -\delta_1\mathbf{I} & \mathbf{0} \\ * & * & * & * & -\delta_1^{-1}\mathbf{I} \end{bmatrix} < 0 \quad (24)$$

where

$$\hat{\mathbf{\Pi}}_{11} = (\mathbf{A}(t)+\mathbf{B}(t)\mathbf{K})^T\mathbf{p}+\mathbf{p}(\mathbf{A}(t)+\mathbf{B}(t)\mathbf{K})$$
$$\hat{\mathbf{\Pi}}_{13} = \hat{\mathbf{\Pi}}_{15} = (\mathbf{C}_1(t)+\mathbf{D}_{12}(t)\mathbf{K})^T$$

$\mathbf{\Pi}_3 < 0$ can be expressed as follows

$$\mathbf{\Pi}_3 = \begin{bmatrix} \hat{\mathbf{\Pi}}_{11} & \mathbf{p}\,\mathbf{D}(t) & \hat{\mathbf{\Pi}}_{13} & \mathbf{0} & \hat{\mathbf{\Pi}}_{15} \\ * & -\gamma^2\mathbf{I} & 0 & \mathbf{F}(t)^T & \mathbf{0} \\ * & * & -\mathbf{I} & \mathbf{0} & \mathbf{0} \\ * & * & * & -\delta_1\mathbf{I} & \mathbf{0} \\ * & * & * & * & -\delta_1^{-1}\mathbf{I} \end{bmatrix} + \begin{bmatrix} \mathbf{0} \\ \mathbf{F}(t)^T \\ \mathbf{0} \\ \mathbf{0} \\ \mathbf{0} \end{bmatrix} \mathbf{I} \begin{bmatrix} \mathbf{0} & \mathbf{F}(t) & \mathbf{0} & \mathbf{0} & \mathbf{0} \end{bmatrix} < 0 \quad (25)$$

By using Lemma 2, $\mathbf{\Pi}_3 < 0$ is equivalent to

$$\mathbf{\Pi}_4 = \begin{bmatrix} \hat{\mathbf{\Pi}}_{11} & \mathbf{p}\,\mathbf{D}(t) & \hat{\mathbf{\Pi}}_{13} & \mathbf{0} & \hat{\mathbf{\Pi}}_{15} & \mathbf{0} \\ * & -\gamma^2\mathbf{I} & 0 & \mathbf{F}(t)^T & \mathbf{0} & \mathbf{F}(t)^T \\ * & * & -\mathbf{I} & \mathbf{0} & \mathbf{0} & \mathbf{0} \\ * & * & * & -\delta_1\mathbf{I} & \mathbf{0} & \mathbf{0} \\ * & * & * & * & -\delta_1^{-1}\mathbf{I} & \mathbf{0} \\ * & * & * & * & * & -\mathbf{I} \end{bmatrix} < 0 \quad (26)$$

Pre- and post-multiplying Equation (26) by $diag\left(\mathbf{p}^{-1}, \mathbf{I}, \mathbf{I}, \mathbf{I}, \mathbf{I}, \mathbf{I}\right)$ and its transpose (Congruent transformation), respectively, we obtain

$$\mathbf{\Pi}_5 = \begin{bmatrix} \hat{\mathbf{\Theta}}_{11} & \mathbf{D}(t) & \hat{\mathbf{\Theta}}_{13} & \mathbf{0} & \hat{\mathbf{\Theta}}_{15} & \mathbf{0} \\ * & -\gamma^2\mathbf{I} & \mathbf{0} & \mathbf{F}(t)^T & \mathbf{0} & \mathbf{F}(t)^T \\ * & * & -\mathbf{I} & \mathbf{0} & \mathbf{0} & \mathbf{0} \\ * & * & * & -\delta_1\mathbf{I} & \mathbf{0} & \mathbf{0} \\ * & * & * & * & -\delta_1^{-1}\mathbf{I} & \mathbf{0} \\ * & * & * & * & * & -\mathbf{I} \end{bmatrix} < 0 \tag{27}$$

where

$$\hat{\mathbf{\Theta}}_{11} = \mathbf{A}(t)\mathbf{p}^{-1} + \mathbf{p}^{-1}\mathbf{A}(t)^T + \mathbf{p}^{-1}\mathbf{K}^T\mathbf{B}(t)^T + \mathbf{B}(t)\mathbf{K}\mathbf{p}^{-1}$$
$$\hat{\mathbf{\Theta}}_{13} = \hat{\mathbf{\Theta}}_{15} = \mathbf{p}^{-1}\mathbf{C}_1(t)^T + \mathbf{p}^{-1}\mathbf{K}^T\mathbf{D}_{12}(t)^T$$

After substituting $\mathbf{X} = \mathbf{p}^{-1}, \mathbf{Y} = \mathbf{K}\mathbf{p}^{-1}$ into Equation (27), we acquire

$$\mathbf{\Pi}_5 = \begin{bmatrix} \hat{\mathbf{\Gamma}}_{11} & \mathbf{D}(t) & \hat{\mathbf{\Gamma}}_{13} & \mathbf{0} & \hat{\mathbf{\Gamma}}_{15} & \mathbf{0} \\ * & -\gamma^2\mathbf{I} & \mathbf{0} & \mathbf{F}(t)^T & \mathbf{0} & \mathbf{F}(t)^T \\ * & * & -\mathbf{I} & \mathbf{0} & \mathbf{0} & \mathbf{0} \\ * & * & * & -\delta_1\mathbf{I} & \mathbf{0} & \mathbf{0} \\ * & * & * & * & -\delta_1^{-1}\mathbf{I} & \mathbf{0} \\ * & * & * & * & * & -\mathbf{I} \end{bmatrix} < 0 \tag{28}$$

where

$$\hat{\mathbf{\Gamma}}_{11} = \mathbf{A}(t)\mathbf{X} + \mathbf{X}\mathbf{A}(t)^T + \mathbf{Y}^T\mathbf{B}(t)^T + \mathbf{B}(t)\mathbf{Y}$$
$$\hat{\mathbf{\Gamma}}_{13} = \hat{\mathbf{\Gamma}}_{15} = \mathbf{X}\mathbf{C}_1(t)^T + \mathbf{Y}^T\mathbf{D}_{12}(t)^T$$

Noting Equation (9), we can separate Equation (28) to the certain and uncertain parts, that is

$$\mathbf{\Pi}_5 = \begin{bmatrix} \hat{\mathbf{\Omega}}_{11} & \mathbf{D} & \hat{\mathbf{\Omega}}_{13} & \mathbf{0} & \hat{\mathbf{\Omega}}_{13} & \mathbf{0} \\ * & -\gamma^2\mathbf{I} & \mathbf{0} & \mathbf{F}^T & \mathbf{0} & \mathbf{F}^T \\ * & * & -\mathbf{I} & \mathbf{0} & \mathbf{0} & \mathbf{0} \\ * & * & * & -\delta_1\mathbf{I} & \mathbf{0} & \mathbf{0} \\ * & * & * & * & -\delta_1^{-1}\mathbf{I} & \mathbf{0} \\ * & * & * & * & * & -\mathbf{I} \end{bmatrix} + \begin{bmatrix} \hat{\mathbf{\Psi}}_{11} & \Delta\mathbf{D}(t) & \hat{\mathbf{\Psi}}_{13} & \mathbf{0} & \hat{\mathbf{\Psi}}_{15} & \mathbf{0} \\ * & \mathbf{0} & \mathbf{0} & \Delta\mathbf{F}(t)^T & \mathbf{0} & \Delta\mathbf{F}(t)^T \\ * & * & \mathbf{0} & \mathbf{0} & \mathbf{0} & \mathbf{0} \\ * & * & * & \mathbf{0} & \mathbf{0} & \mathbf{0} \\ * & * & * & * & \mathbf{0} & \mathbf{0} \\ * & * & * & * & * & \mathbf{0} \end{bmatrix} < 0 \tag{29}$$

where

$$\hat{\mathbf{\Omega}}_{11} = \mathbf{A}\mathbf{X} + \mathbf{X}\mathbf{A}^T + \mathbf{Y}^T\mathbf{B}^T + \mathbf{B}\mathbf{Y}$$
$$\hat{\mathbf{\Omega}}_{13} = \hat{\mathbf{\Omega}}_{15} = \mathbf{X}\mathbf{C}_1{}^T + \mathbf{Y}^T\mathbf{D}_{12}{}^T$$
$$\hat{\mathbf{\Psi}}_{11} = \Delta\mathbf{A}(t)\mathbf{X} + \mathbf{X}\Delta\mathbf{A}(t)^T + \mathbf{Y}^T\Delta\mathbf{B}(t)^T + \Delta\mathbf{B}(t)\mathbf{Y}$$
$$\hat{\mathbf{\Psi}}_{13} = \hat{\mathbf{\Psi}}_{15} = \mathbf{X}\Delta\mathbf{C}_1(t)^T + \mathbf{Y}^T\Delta\mathbf{D}_{12}(t)^T$$

By using Equation (10), it is easily obtained that

$$\begin{cases} \Delta\mathbf{A}(t) = \mathbf{M}_A\mathbf{E}(t)\mathbf{N}_A \\ \Delta\mathbf{B}(t) = \mathbf{M}_B\mathbf{E}(t)\mathbf{N}_B \\ \Delta\mathbf{D}(t) = \mathbf{M}_D\mathbf{E}(t)\mathbf{N}_D \\ \Delta\mathbf{C}_1(t) = \mathbf{M}_{C_1}\mathbf{E}(t)\mathbf{N}_{C_1} \\ \Delta\mathbf{D}_{12}(t) = \mathbf{M}_{D_{12}}\mathbf{E}(t)\mathbf{N}_{D_{12}} \\ \Delta\mathbf{F}(t) = \mathbf{M}_F\mathbf{E}(t)\mathbf{N}_F \end{cases} \tag{30}$$

If we substitute Equation (30) into the uncertain part of Equation (29) and then use Lemma 1, we can find the upper bound for each element as follows

$$\begin{aligned}\Xi_1 &= \begin{bmatrix} \Delta\mathbf{A}(t)\mathbf{X}+\mathbf{X}\Delta\mathbf{A}(t)^T & \mathbf{0} & \mathbf{0} & \mathbf{0} & \mathbf{0} & \mathbf{0} \\ \mathbf{0} & \mathbf{0} & \mathbf{0} & \mathbf{0} & \mathbf{0} & \mathbf{0} \\ \mathbf{0} & \mathbf{0} & \mathbf{0} & \mathbf{0} & \mathbf{0} & \mathbf{0} \\ \mathbf{0} & \mathbf{0} & \mathbf{0} & \mathbf{0} & \mathbf{0} & \mathbf{0} \\ \mathbf{0} & \mathbf{0} & \mathbf{0} & \mathbf{0} & \mathbf{0} & \mathbf{0} \\ \mathbf{0} & \mathbf{0} & \mathbf{0} & \mathbf{0} & \mathbf{0} & \mathbf{0} \end{bmatrix} = \begin{bmatrix} \mathbf{M}_A \\ \mathbf{0} \\ \mathbf{0} \\ \mathbf{0} \\ \mathbf{0} \\ \mathbf{0} \end{bmatrix} \mathbf{E}(t) \begin{bmatrix} \mathbf{N}_A\mathbf{X} & \mathbf{0} & \mathbf{0} & \mathbf{0} & \mathbf{0} & \mathbf{0} \end{bmatrix} + \begin{bmatrix} \mathbf{X}\mathbf{N}_A^T \\ \mathbf{0} \\ \mathbf{0} \\ \mathbf{0} \\ \mathbf{0} \\ \mathbf{0} \end{bmatrix} \mathbf{E}(t) \begin{bmatrix} \mathbf{M}_A^T & \mathbf{0} & \mathbf{0} & \mathbf{0} & \mathbf{0} & \mathbf{0} \end{bmatrix} \\ &\leq \underbrace{\begin{bmatrix} \mathbf{M}_A \\ \mathbf{0} \\ \mathbf{0} \\ \mathbf{0} \\ \mathbf{0} \\ \mathbf{0} \end{bmatrix} \varepsilon_1 \begin{bmatrix} \mathbf{M}_A^T & \mathbf{0} & \mathbf{0} & \mathbf{0} & \mathbf{0} & \mathbf{0} \end{bmatrix}}_{LMI} + \underbrace{\begin{bmatrix} \mathbf{X}\mathbf{N}_A^T \\ \mathbf{0} \\ \mathbf{0} \\ \mathbf{0} \\ \mathbf{0} \\ \mathbf{0} \end{bmatrix} \varepsilon_1^{-1} \begin{bmatrix} \mathbf{N}_A\mathbf{X} & \mathbf{0} & \mathbf{0} & \mathbf{0} & \mathbf{0} & \mathbf{0} \end{bmatrix}}_{\Omega_1}\end{aligned} \quad (31)$$

You can find others in Appendix A from Equation (A1) to Equation (A8). By adding LMI parts of Equations (31) and (A1)–(A8) to the constant part of Equation (29), we have

$$\boldsymbol{\Pi}_5 = \bar{\boldsymbol{\Xi}} + \sum_{1}^{9} \boldsymbol{\Omega}_i < 0 \quad (32)$$

where $\bar{\boldsymbol{\Xi}}$ is the same in Equation (13). Eventually, by applying Lemma 2 to each Ω_i with $i = 1, \ldots, 9$, we can construct an LMI in the form of Equation (13). Conditions $\mathbf{X} > 0$, $\varepsilon_i > 0$ with $i = 1, \ldots, 9$, and Equation (13) guarantee $\Pi_1 < 0$, which further implies that $J_\infty < 0$ in Equation (15), and therefore $\|\mathbf{z}(t)\|^2_{\mathcal{L}_2} < \gamma^2 \|\mathbf{v}(t)\|^2_{\mathcal{L}_2}$. In the actual implementation of the control systems (including active suspension systems), the direct effects of high gain control can lead to some major problems such as actuator saturation and noise amplification. Therefore, the gain matrix $\mathbf{K}$ should be limited. In this study, we use the same approach that was employed to solve this problem in [2]. Accordingly, conforming to expression $\mathbf{K} = \mathbf{Y}\mathbf{X}^{-1}$, restriction of the size of the gain matrix $\mathbf{K}$ is possible by constraining the two matrices $\mathbf{Y}$ and $\mathbf{X}^{-1}$. We assigned

$$\mathbf{Y}^T\mathbf{Y} < L_R\mathbf{I}, \quad L_R > 0 \quad (33)$$

$$\mathbf{X}^{-1} < L_S\mathbf{I}, \quad L_S > 0 \quad (34)$$

Utilizing Lemma 2 (Schur complement), LMIs in Equations (33) and (34) lead to the LMIs in Equations (14) and (15), respectively. Therefore, the proof of Theorem 1 is completed. □

The active vehicle suspension system without inerter and uncertainty can be defined by the following state-space equations [2]:

$$\begin{aligned} \dot{\mathbf{x}}(t) &= \bar{\mathbf{A}}\mathbf{x}(t) + \bar{\mathbf{B}}\mathbf{u}(t) + \bar{\mathbf{D}}\mathbf{v}(t) \\ \mathbf{z}(t) &= \bar{\mathbf{C}}_1\mathbf{x}(t) + \bar{\mathbf{D}}_{12}\mathbf{u}(t) \\ \mathbf{y}(t) &= \bar{\mathbf{C}}_2\mathbf{x}(t) \end{aligned} \quad (35)$$

Corollary 1 introduces a robust H_∞ controller, where without external disturbance, the closed-loop system evolves asymptotically stable, and in the existence of external disturbance, the desired amount of disturbance attenuation is acquired.

Corollary 1. *Supposing positive constants $\bar{\gamma}$, $\bar{L}_R$, and $\bar{L}_S$, the linear active suspension system in Equation (35) with state-feedback controller ($\mathbf{u}(t) = \mathbf{K}_{II}\mathbf{x}(t)$), is asymptotically stable without external disturbance, and in the existence of external disturbance fulfills $\|\mathbf{z}(t)\|^2_{\mathcal{L}_2} < \bar{\gamma}^2\|\mathbf{v}(t)\|^2_{\mathcal{L}_2}$ for $\mathbf{v}(t) \in \mathcal{L}_2[\ 0 \quad \infty\ )$, if there exist symmetric positive definite matrix $\bar{\mathbf{X}} > 0$ and matrix $\bar{\mathbf{Y}}$ with appropriate dimensions such that the following LMIs hold*

$$\begin{bmatrix} \bar{\mathbf{A}}\bar{\mathbf{X}} + \bar{\mathbf{X}}\bar{\mathbf{A}}^T + \bar{\mathbf{Y}}^T\bar{\mathbf{B}}^T + \bar{\mathbf{B}}\bar{\mathbf{Y}} & \bar{\mathbf{D}} & \bar{\mathbf{X}}\bar{\mathbf{C}}_1^T + \bar{\mathbf{Y}}^T\bar{\mathbf{D}}_{12}^T \\ * & -\bar{\gamma}^2\mathbf{I} & \mathbf{0} \\ * & * & -\mathbf{I} \end{bmatrix} < 0 \quad (36)$$

$$\begin{bmatrix} \bar{L}_R\mathbf{I} & \bar{\mathbf{Y}}^T \\ \bar{\mathbf{Y}} & \mathbf{I} \end{bmatrix} > 0 \quad (37)$$

$$\begin{bmatrix} \bar{L}_S\mathbf{I} & \mathbf{I} \\ \mathbf{I} & \bar{\mathbf{X}} \end{bmatrix} > 0 \tag{38}$$

4. Application to Active Inerter-Based Quarter-Car Suspension System

In this section, we will apply the proposed method to the active inerter-based quarter-car suspension system described in Section 2 to illustrate the effectiveness of the proposed robust H_∞ controller method. The parameters of the active inerter-based suspension system for the quarter-car model are listed in Table 1.

Table 1. System parameter values of the active inerter-based quarter-car suspension system.

Parameter	Value
$m_s(t)$	972.2 ± 145.83 kg
m_u	113.6 kg
k_s	42,719.6 N/m
c_s	1095 Ns/m
$b_s(t)$	52.5 ± 2.5 kg
k_t	101,115 N/m
c_t	14.6 Ns/m

Note that in our simulations we assume that m_s and b_s are uncertain. We use a variable mass profile (15% sprung mass uncertainty) and a continuous uniform random distribution for the inertance of inerter (10% inertance uncertainty) to generate them, as shown in Figure 3.

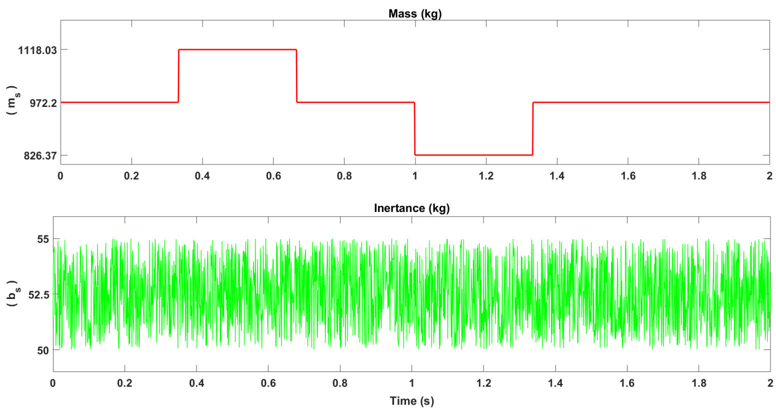

Figure 3. The variable mass and interance of active inerter-based suspension system.

By setting $\gamma = 9$, $\delta_1 = 0.01$, $L_R = 10^6$, $L_s = 10^3$, $\alpha = 15$, $\beta = 22$, $\rho = 0.6$, and solving the convex optimization problem formulated in Theorem 1 using the YALMIP toolbox [28], the gain matrix of controller is acquired as follows

$$\mathbf{K} = \begin{bmatrix} -4989 & 12076 & -9141.9 & -209 \end{bmatrix}$$

And for brevity, we will indicate the proposed controller as Controller **I** hereafter.

To assess the performance of the proposed Controller **I**, the acquired results are compared with those obtained with a robust H_∞ control for the active vehicle suspension without inerter, which is marked as Controller **II** for brevity. By using Corollary 1, and according to these design parameters $\bar{\gamma} = 9$, $\bar{L}_R = 10^6$, $\bar{L}_s = 10^4$, $\bar{\alpha} = 21$, $\bar{\beta} = 42$, $\bar{\rho} = 1.1$, Controller **II** gain achieved as follows

$$\mathbf{K}_{II} = \begin{bmatrix} -2422.5 & -11368 & -12865 & 171.71 \end{bmatrix}$$

According to ISO 2361, reducing the vertical acceleration of a vehicle system in the frequency range of 4 to 8 Hz is equivalent to improving ride comfort. Therefore, we first concentrate on the frequency responses from ground velocity to vertical body acceleration for the passive and active suspension systems employing the robust H_∞ state-feedback controllers. From Figure 4, we can see that the desired controller **I** and the controller **II** can provide the lower value of the H_∞ norm over the frequency range of 4–8Hz.

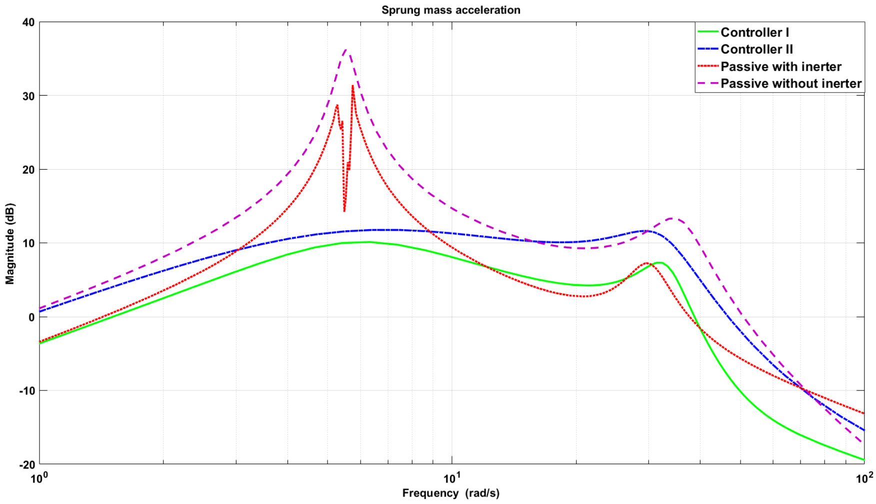

Figure 4. Frequency responses for the open- and closed-loop systems.

Performance of the quarter-car suspension system is capable to be assessed by examining three response quantities, that is, the sprung mass acceleration $\dot{x}_3(t)$, suspension deflection $x_1(t)$, and tire deflection $x_2(t)$. In the following subsections, we will utilize Shock (Bump) and Vibration (Rough Road) road profiles to investigate the performance of the quarter-car suspension system in regard to the ride comfort, vehicle handling, and energy consumption of the suspension.

4.1. Bump Response

Here, a bump or pothole with a relatively short duration and high intensity confronted on a flat surface characterizes the transient response, which is given by

$$z_{rf}(t) = \begin{cases} \frac{a}{2}\left(1 - \cos(\frac{2\pi v_0}{l}t)\right) & ,0 \le t \le \frac{l}{v_0} \\ 0 & ,t > \frac{l}{v_0} \end{cases} \tag{39}$$

where a and l denote the height and length of the bump profile. We select $a = 0.1$ m, $l = 2$ m, and the forward velocity of the vehicle chosen as $v_0 = 18$ km/h .

The response of the quarter-car suspension system with inerter by using Controller **I** and without inerter by using Controller **II**, and passive suspension are compared in Figure 5. Figure 5 displays the sprung mass acceleration, suspension deflection, and tire deflection. The control effort of the active controllers is also plotted in Figure 6. It can be seen from Figure 5 that the Controllers **I** and **II** compared to the passive suspension system acquire better responses. The simulation results confirm that the active suspension system with inerter is better than the active suspension without inerter with respect to all performance criteria for the bump disturbance. On the other hand, compared to Controller **I**, more control effort is required for Controller **II**, which is shown in Figure 6.

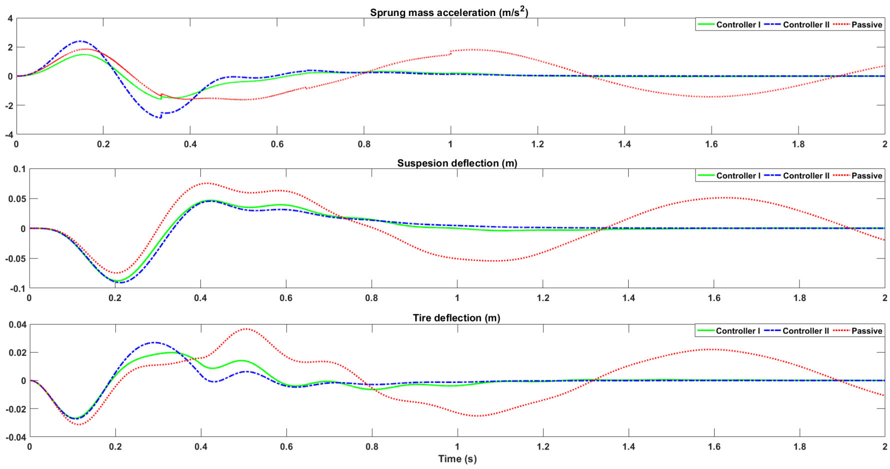

Figure 5. Sprung mass acceleration, suspension deflection, and tire deflection for the bump road profile.

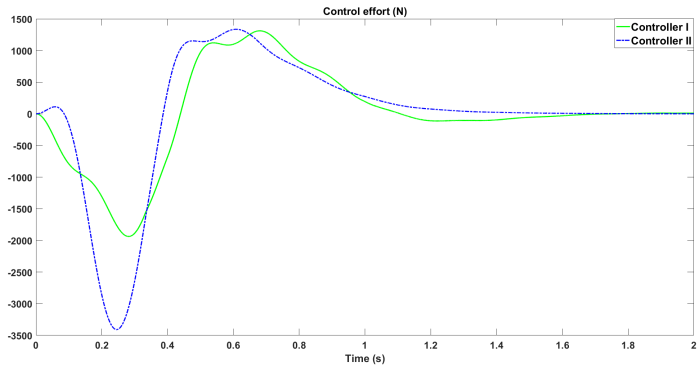

Figure 6. Control effort required for the Controllers **I** and **II**.

In order to qualitatively assess the control effort, the following $\mathcal{L}_2$ norm value is employed to determine the energy consumption of two active control methods:

$$\|\mathbf{u}(t)\|_{\mathcal{L}_2} = \sqrt{\int_0^{\bar{T}} \mathbf{u}(t)^T \mathbf{u}(t) dt} \quad (40)$$

where $\bar{T} = 2\,s$ denotes the simulation time. Energy consumption of two controllers is shown in Table 2. This table shows that the control effort of the active inerter-based suspension system with Controller **I** is lower than that of the active suspension system without inerter. Consequently, the low gain of the Controller **I** results in lower energy consumption.

Table 2. Assessment of energy consumption for active controllers.

	Controller I	**Controller II**
Energy consumption	1051.3	1424.2

4.2. Random Response

Generally, it is capable to assume random vibrations as road disturbances, which are consistent and frequently described as a random process. The ground displacement power spectral density (PSD) is defined as follows

$$S_g(\Omega) = \begin{cases} S_g(\Omega_0)(\frac{\Omega}{\Omega_0})^{-n_1} & if \;\; \Omega \leq \Omega_0 \\ S_g(\Omega_0)(\frac{\Omega}{\Omega_0})^{-n_2} & if \;\; \Omega > \Omega_0 \end{cases} \quad (41)$$

where $\Omega_0 = 1/2\pi$ stands for reference spatial frequency and Ω is a spatial frequency. The value of $S_g(\Omega_0)$ denotes a measure for the roughness coefficient of the road. n_1 and n_2 represent the road roughness constants.

In particular, if the vehicle is presumed to be moving at a constant horizontal speed v_0 over a given road, it is capable to simulate the force caused by the road irregularities using the following series

$$z_r f(t) = \sum_{n=1}^{N} s_n \sin(n\omega_0 t + \varphi_n) \tag{42}$$

where $s_n = \sqrt{2s_g(n\Delta\Omega)\Delta\Omega}$, $\Delta\Omega = 2\pi/L$, and L is the length of the road segment considered. The amplitudes s_n of the excitation harmonics are assessed from the road spectra selected. Additionally, the value of the fundamental temporal frequency ω_0 is calculated from $\omega_0 = \frac{2\pi}{L}v_0$. Whereas the phases φ_n are considered as random variables with a uniform distribution in the range $[0, 2\pi)$.

According to $ISO2631$ standards, road class D (poor quality) $\left(S_g(\Omega_0) = 256 \times 10^{-6}\ \text{m}^3\right)$, and road class E (very poor quality) $\left(S_g(\Omega_0) = 1024 \times 10^{-6}\ \text{m}^3\right)$, are chosen as a standard road profile. In this paper, $n_1 = 2, n_2 = 1.5, L = 100, N_f = 200$ and the horizontal speed $v_0 = 36$ m/s, are utilized to generate the random road profiles as shown in Figure 7.

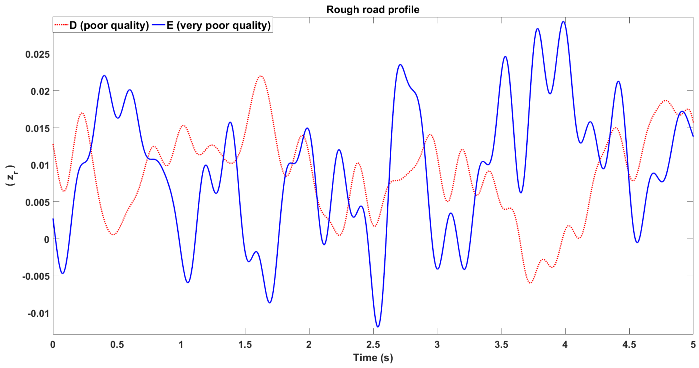

Figure 7. A case in point of random road profiles (class D (poor quality), class E (very poor quality)).

The random response of the active inerter-based quarter-car suspension system for two road class profiles are compared in Figures 8 and 9. These figures display the sprung mass acceleration, suspension deflection, and tire deflection. It can be seen from Figures 8 and 9 that the Controllers **I** and **II** compared to the passive suspension system acquire better responses. It is confirmed by the simulation results that random response quantities for all performance requirements of active inerter-based suspension system are better than active suspension without inerter.

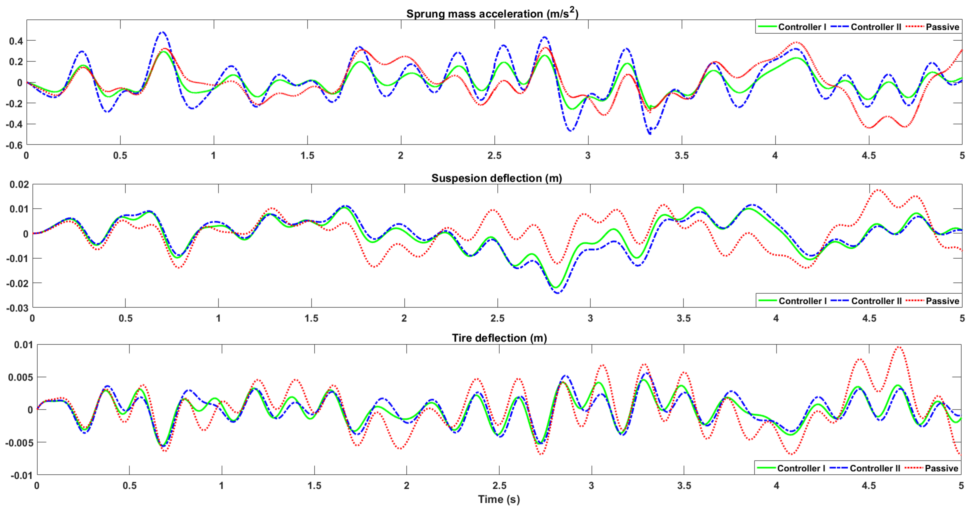

Figure 8. Sprung mass acceleration, suspension deflection, and tire deflection with the class D (poor quality) road profile.

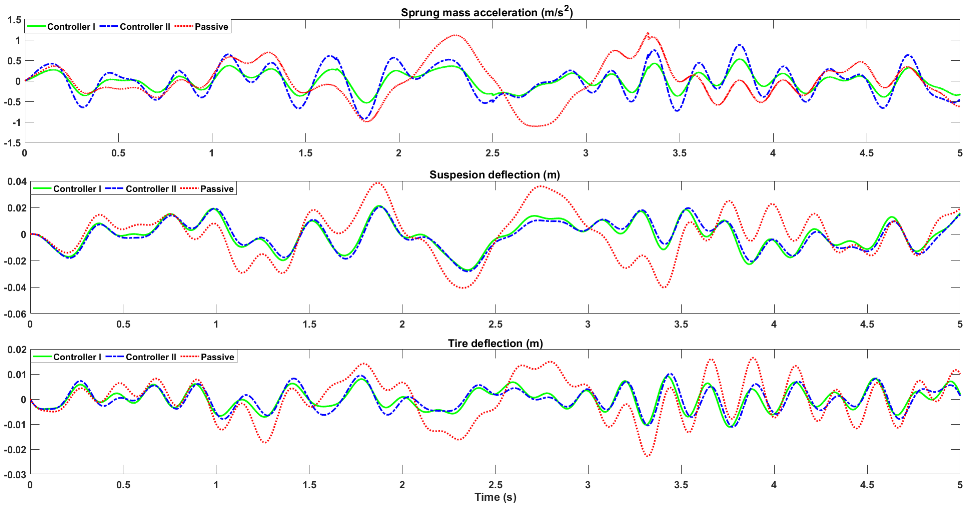

Figure 9. Sprung mass acceleration, suspension deflection, and tire deflection with the class E (very poor quality) road profile.

To assess the probabilistic properties of the random response, the Monte Carlo simulation is utilized. Therefore, taking into consideration the random variable φ_n of the excitation applied, the performance index of the Root Mean Square (RMS) is determined by the expected values:

$$J_1 = \mathrm{E}\left[\frac{1}{\bar{T}}\int_0^{\bar{T}}[\dot{x}_3(t)]^2 dt\right] \tag{43}$$

$$J_2 = \mathrm{E}\left[\frac{1}{\bar{T}}\int_0^{\bar{T}}[x_1(t)]^2 dt\right] \tag{44}$$

$$J_3 = \mathrm{E}\left[\frac{1}{\bar{T}}\int_0^{\bar{T}}[x_2(t)]^2 dt\right] \tag{45}$$

J_1 for the sprung mass acceleration, J_2 for suspension deflection, and J_3 for tire deflection have been considered; where $\bar{T} = L/v_0$ is the temporal measurement period. For calculating RMS values, we have considered $\bar{T} = 5$ in Equations (43)–(45) and the simulation has been run randomly 100 times.

To validate the effectiveness of controller **I** in dealing with the active suspension system based on inerter, the RMS ratios $J_{II_i}(t)/J_{I_i}(t)$, $J_{P_i}(t)/J_{I_i}(t)$, $i = 1, 2, 3$, are calculated, where $J_{I_i}(t)$ represents the RMS value of the active suspension system with inerter by using Controller **I**, $J_{II_i}(t)$ denotes the RMS value of the active suspension system without inerter by using Controller **II**, and $J_{P_i}(t)$ is the RMS value of the passive suspension system.

Tables 3 and 4 represent the results of RMS ratios for Controller **I**, Controller **II**, and passive suspension system for the poor (class D) and very poor (class E) quality road profile. Tables 3 and 4 additionally display the control efforts of the active controllers.

It can be seen from Tables 3 and 4 that the RMS ratios of the active inerter-based suspension system with Controllers **I** for all performance requirements (sprung mass acceleration, suspension deflection, and tire deflection) acquire better response compared to both Controller **II** and passive suspension system (the response ratio is more than 1). In addition, the required control effort for Controller **I** is less than for Controller **II**.

Table 3. Energy consumption and RMS values of random road profile (Class D).

Performance Criteria	$J_{II_i}(t)/J_{I_i}(t)$	$J_{P_i}(t)/J_{I_i}(t)$	
Sprung mass acceleration	2.7985	3.6151	
Suspension deflection	1.1586	2.1501	
Tire deflection	1.7552	3.7421	
	Pasive	Controller I	Controller II
Energy consumption	—	478.55	627.91

Table 4. Energy consumption and RMS values of random road profile (Class E).

Performance Criteria	$J_{II_i}(t)/J_{I_i}(t)$	$J_{P_i}(t)/J_{I_i}(t)$	
Sprung mass acceleration	2.8693	4.734	
Suspension deflection	1.0827	2.7508	
Tire deflection	1.7615	3.9997	
	Pasive	Controller I	Controller II
Energy consumption	—	677.2	917.7

5. Conclusions

In this paper, the performance of the active inerter-based quarter-car suspension system in the present of parameter uncertainties and external disturbance is investigated. A robust H_∞ controller is developed to optimize the H_∞ norm of the active suspension system to enhance the ride comfort, suspension deflections and tire loads. Furthermore, two more LMIs are added to the established sufficient conditions in order to limit the gain of the controller. Finally, to validate the effectiveness of the proposed approach, it is applied to the quarter-car model to minimize the influence of parameter uncertainty and road disturbance on the suspension system performance. It was observed that the active inerter-based suspension system for all performance requirements achieve better response compared to both active suspension without inerter and passive suspension with inerter. Therefore, the presence of inerter in the dynamics of the vehicle suspension system not only improves the performance requirements, but also reduces the control effort of the actuator. It is noteworthy that by employing advanced inerter, it is possible to supply some of the energy required to operate the actuator. The proposed approach is expected to pave the way for the application of theoretical discoveries to practical vehicle suspension systems. Furthermore, an adaptive inerter can attenuate the amplitude of vibration of the damped body over a much wider range of excitation frequency. In future work, a non-fixed inerter will be employed as a variable element in the semi-active suspension system that can be adjusted in real-time.

Author Contributions: Conceptualization, K.K.A., R.K. and J.K.; methodology, K.K.A.; software, K.K.A.; validation, K.K.A., R.K. and J.K.; formal analysis, K.K.A.; investigation, K.K.A.; resources, K.K.A.; data curation, K.K.A.; writing—original draft preparation, K.K.A.; writing—review and editing, K.K.A., R.K. and J.K; visualization, K.K.A.; supervision, K.K.A. and J.K.; project administration, K.K.A. All authors have read and agreed to the published version of the manuscript.

Funding: This research received no external funding.

Data Availability Statement: The data presented in this study are available on request from the corresponding author. The data are not publicly available due to restrictions, e.g., privacy or ethics and using special solvers to solve the convex optimization problem.

Acknowledgments: K. Karim Afshar would like to appreciate Ali Javadi https://scholar.google.com/citations?user=1sj6lvwAAAAJ&hl=en for his valuable training and guidance that led to scientific progress in writing this article.

Conflicts of Interest: The authors declare no conflict of interest.

Appendix A

$$
\begin{aligned}
\Xi_2 &= \begin{bmatrix} \Delta\mathbf{B}(t)\mathbf{Y}+\mathbf{Y}^T\Delta\mathbf{B}(t)^T & \mathbf{0} & \mathbf{0} & \mathbf{0} & \mathbf{0} & \mathbf{0} \\ \mathbf{0} & \mathbf{0} & \mathbf{0} & \mathbf{0} & \mathbf{0} & \mathbf{0} \\ \mathbf{0} & \mathbf{0} & \mathbf{0} & \mathbf{0} & \mathbf{0} & \mathbf{0} \\ \mathbf{0} & \mathbf{0} & \mathbf{0} & \mathbf{0} & \mathbf{0} & \mathbf{0} \\ \mathbf{0} & \mathbf{0} & \mathbf{0} & \mathbf{0} & \mathbf{0} & \mathbf{0} \\ \mathbf{0} & \mathbf{0} & \mathbf{0} & \mathbf{0} & \mathbf{0} & \mathbf{0} \end{bmatrix} = \begin{bmatrix} \mathbf{M}_B \\ \mathbf{0} \\ \mathbf{0} \\ \mathbf{0} \\ \mathbf{0} \\ \mathbf{0} \end{bmatrix} \mathbf{E}(t) \begin{bmatrix} \mathbf{N}_B\mathbf{Y} & \mathbf{0} & \mathbf{0} & \mathbf{0} & \mathbf{0} & \mathbf{0} \end{bmatrix} + \begin{bmatrix} \mathbf{Y}^T\mathbf{N}_B^T \\ \mathbf{0} \\ \mathbf{0} \\ \mathbf{0} \\ \mathbf{0} \\ \mathbf{0} \end{bmatrix} \mathbf{E}(t) \begin{bmatrix} \mathbf{M}_B^T & \mathbf{0} & \mathbf{0} & \mathbf{0} & \mathbf{0} & \mathbf{0} \end{bmatrix} \\
&\leq \underbrace{\begin{bmatrix} \mathbf{M}_B \\ \mathbf{0} \\ \mathbf{0} \\ \mathbf{0} \\ \mathbf{0} \\ \mathbf{0} \end{bmatrix} \varepsilon_2 \begin{bmatrix} \mathbf{M}_B^T & \mathbf{0} & \mathbf{0} & \mathbf{0} & \mathbf{0} & \mathbf{0} \end{bmatrix}}_{LMI} + \underbrace{\begin{bmatrix} \mathbf{Y}^T\mathbf{N}_B^T \\ \mathbf{0} \\ \mathbf{0} \\ \mathbf{0} \\ \mathbf{0} \\ \mathbf{0} \end{bmatrix} \varepsilon_2^{-1} \begin{bmatrix} \mathbf{N}_B\mathbf{Y} & \mathbf{0} & \mathbf{0} & \mathbf{0} & \mathbf{0} & \mathbf{0} \end{bmatrix}}_{\mathbf{\Omega}_2}
\end{aligned} \tag{A1}
$$

$$
\begin{aligned}
\Xi_3 &= \begin{bmatrix} \mathbf{0} & \Delta\mathbf{D}(t) & \mathbf{0} & \mathbf{0} & \mathbf{0} & \mathbf{0} \\ \Delta\mathbf{D}(t)^T & \mathbf{0} & \mathbf{0} & \mathbf{0} & \mathbf{0} & \mathbf{0} \\ \mathbf{0} & \mathbf{0} & \mathbf{0} & \mathbf{0} & \mathbf{0} & \mathbf{0} \\ \mathbf{0} & \mathbf{0} & \mathbf{0} & \mathbf{0} & \mathbf{0} & \mathbf{0} \\ \mathbf{0} & \mathbf{0} & \mathbf{0} & \mathbf{0} & \mathbf{0} & \mathbf{0} \\ \mathbf{0} & \mathbf{0} & \mathbf{0} & \mathbf{0} & \mathbf{0} & \mathbf{0} \end{bmatrix} = \begin{bmatrix} \mathbf{M}_D \\ \mathbf{0} \\ \mathbf{0} \\ \mathbf{0} \\ \mathbf{0} \\ \mathbf{0} \end{bmatrix} \mathbf{E}(t) \begin{bmatrix} \mathbf{0} & \mathbf{N}_D & \mathbf{0} & \mathbf{0} & \mathbf{0} & \mathbf{0} \end{bmatrix} + \begin{bmatrix} \mathbf{0} \\ \mathbf{N}_D^T \\ \mathbf{0} \\ \mathbf{0} \\ \mathbf{0} \\ \mathbf{0} \end{bmatrix} \mathbf{E}(t) \begin{bmatrix} \mathbf{M}_D^T & \mathbf{0} & \mathbf{0} & \mathbf{0} & \mathbf{0} & \mathbf{0} \end{bmatrix} \\
&\leq \underbrace{\begin{bmatrix} \mathbf{M}_D \\ \mathbf{0} \\ \mathbf{0} \\ \mathbf{0} \\ \mathbf{0} \\ \mathbf{0} \end{bmatrix} \varepsilon_3 \begin{bmatrix} \mathbf{M}_D^T & \mathbf{0} & \mathbf{0} & \mathbf{0} & \mathbf{0} & \mathbf{0} \end{bmatrix}}_{LMI} + \underbrace{\begin{bmatrix} \mathbf{0} \\ \mathbf{N}_D^T \\ \mathbf{0} \\ \mathbf{0} \\ \mathbf{0} \\ \mathbf{0} \end{bmatrix} \varepsilon_3^{-1} \begin{bmatrix} \mathbf{0} & \mathbf{N}_D & \mathbf{0} & \mathbf{0} & \mathbf{0} & \mathbf{0} \end{bmatrix}}_{\mathbf{\Omega}_3}
\end{aligned} \tag{A2}
$$

$$
\begin{aligned}
\Xi_4 &= \begin{bmatrix} \mathbf{0} & \mathbf{0} & \mathbf{X}\Delta\mathbf{C}_1(t)^T & \mathbf{0} & \mathbf{0} & \mathbf{0} \\ \mathbf{0} & \mathbf{0} & \mathbf{0} & \mathbf{0} & \mathbf{0} & \mathbf{0} \\ \Delta\mathbf{C}_1(t)\mathbf{X} & \mathbf{0} & \mathbf{0} & \mathbf{0} & \mathbf{0} & \mathbf{0} \\ \mathbf{0} & \mathbf{0} & \mathbf{0} & \mathbf{0} & \mathbf{0} & \mathbf{0} \\ \mathbf{0} & \mathbf{0} & \mathbf{0} & \mathbf{0} & \mathbf{0} & \mathbf{0} \\ \mathbf{0} & \mathbf{0} & \mathbf{0} & \mathbf{0} & \mathbf{0} & \mathbf{0} \end{bmatrix} = \begin{bmatrix} \mathbf{X}\mathbf{N}_{c_1}^T \\ \mathbf{0} \\ \mathbf{0} \\ \mathbf{0} \\ \mathbf{0} \\ \mathbf{0} \end{bmatrix} \mathbf{E}(t) \begin{bmatrix} \mathbf{0} & \mathbf{0} & \mathbf{M}_{c_1}^T & \mathbf{0} & \mathbf{0} & \mathbf{0} \end{bmatrix} + \begin{bmatrix} \mathbf{0} \\ \mathbf{0} \\ \mathbf{M}_{c_1} \\ \mathbf{0} \\ \mathbf{0} \\ \mathbf{0} \end{bmatrix} \mathbf{E}(t) \begin{bmatrix} \mathbf{N}_{c_1}\mathbf{X} & \mathbf{0} & \mathbf{0} & \mathbf{0} & \mathbf{0} & \mathbf{0} \end{bmatrix} \\
&\leq \underbrace{\begin{bmatrix} \mathbf{0} \\ \mathbf{0} \\ \mathbf{M}_{c_1} \\ \mathbf{0} \\ \mathbf{0} \\ \mathbf{0} \end{bmatrix} \varepsilon_4 \begin{bmatrix} \mathbf{0} & \mathbf{0} & \mathbf{M}_{c_1}^T & \mathbf{0} & \mathbf{0} & \mathbf{0} \end{bmatrix}}_{LMI} + \underbrace{\begin{bmatrix} \mathbf{X}\mathbf{N}_{c_1}^T \\ \mathbf{0} \\ \mathbf{0} \\ \mathbf{0} \\ \mathbf{0} \\ \mathbf{0} \end{bmatrix} \varepsilon_4^{-1} \begin{bmatrix} \mathbf{N}_{c_1}\mathbf{X} & \mathbf{0} & \mathbf{0} & \mathbf{0} & \mathbf{0} & \mathbf{0} \end{bmatrix}}_{\mathbf{\Omega}_4}
\end{aligned} \tag{A3}
$$

$$
\begin{aligned}
\Xi_5 &= \begin{bmatrix} \mathbf{0} & \mathbf{0} & \mathbf{Y}^T\Delta\mathbf{D}_{12}(t)^T & \mathbf{0} & \mathbf{0} & \mathbf{0} \\ \mathbf{0} & \mathbf{0} & \mathbf{0} & \mathbf{0} & \mathbf{0} & \mathbf{0} \\ \Delta\mathbf{D}_{12}(t)\mathbf{Y} & \mathbf{0} & \mathbf{0} & \mathbf{0} & \mathbf{0} & \mathbf{0} \\ \mathbf{0} & \mathbf{0} & \mathbf{0} & \mathbf{0} & \mathbf{0} & \mathbf{0} \\ \mathbf{0} & \mathbf{0} & \mathbf{0} & \mathbf{0} & \mathbf{0} & \mathbf{0} \\ \mathbf{0} & \mathbf{0} & \mathbf{0} & \mathbf{0} & \mathbf{0} & \mathbf{0} \end{bmatrix} = \begin{bmatrix} \mathbf{Y}^T\mathbf{N}_{D_{12}}^T \\ \mathbf{0} \\ \mathbf{0} \\ \mathbf{0} \\ \mathbf{0} \\ \mathbf{0} \end{bmatrix} \mathbf{E}(t) \begin{bmatrix} \mathbf{0} & \mathbf{0} & \mathbf{M}_{D_{12}}^T & \mathbf{0} & \mathbf{0} & \mathbf{0} \end{bmatrix} + \begin{bmatrix} \mathbf{0} \\ \mathbf{0} \\ \mathbf{M}_{D_{12}} \\ \mathbf{0} \\ \mathbf{0} \\ \mathbf{0} \end{bmatrix} \mathbf{E}(t) \begin{bmatrix} \mathbf{N}_{D_{12}}\mathbf{Y} & \mathbf{0} & \mathbf{0} & \mathbf{0} & \mathbf{0} & \mathbf{0} \end{bmatrix} \\
&\leq \underbrace{\begin{bmatrix} \mathbf{0} \\ \mathbf{0} \\ \mathbf{M}_{D_{12}} \\ \mathbf{0} \\ \mathbf{0} \\ \mathbf{0} \end{bmatrix} \varepsilon_5 \begin{bmatrix} \mathbf{0} & \mathbf{0} & \mathbf{M}_{D_{12}}^T & \mathbf{0} & \mathbf{0} & \mathbf{0} \end{bmatrix}}_{LMI} + \underbrace{\begin{bmatrix} \mathbf{Y}^T\mathbf{N}_{D_{12}}^T \\ \mathbf{0} \\ \mathbf{0} \\ \mathbf{0} \\ \mathbf{0} \\ \mathbf{0} \end{bmatrix} \varepsilon_5^{-1} \begin{bmatrix} \mathbf{N}_{D_{12}}\mathbf{Y} & \mathbf{0} & \mathbf{0} & \mathbf{0} & \mathbf{0} & \mathbf{0} \end{bmatrix}}_{\mathbf{\Omega}_5}
\end{aligned} \tag{A4}
$$

$$
\begin{aligned}
\Xi_6 &= \begin{bmatrix} \mathbf{0} & \mathbf{0} & \mathbf{0} & \mathbf{0} & \mathbf{0} & \mathbf{0} \\ \mathbf{0} & \mathbf{0} & \mathbf{0} & \Delta\mathbf{F}(t)^T & \mathbf{0} & \mathbf{0} \\ \mathbf{0} & \mathbf{0} & \mathbf{0} & \mathbf{0} & \mathbf{0} & \mathbf{0} \\ \mathbf{0} & \Delta\mathbf{F}(t) & \mathbf{0} & \mathbf{0} & \mathbf{0} & \mathbf{0} \\ \mathbf{0} & \mathbf{0} & \mathbf{0} & \mathbf{0} & \mathbf{0} & \mathbf{0} \\ \mathbf{0} & \mathbf{0} & \mathbf{0} & \mathbf{0} & \mathbf{0} & \mathbf{0} \end{bmatrix} = \begin{bmatrix} \mathbf{0} \\ \mathbf{N}_F^T \\ \mathbf{0} \\ \mathbf{0} \\ \mathbf{0} \\ \mathbf{0} \end{bmatrix} \mathbf{E}(t) \begin{bmatrix} \mathbf{0} & \mathbf{0} & \mathbf{0} & \mathbf{M}_F^T & \mathbf{0} & \mathbf{0} \end{bmatrix} + \begin{bmatrix} \mathbf{0} \\ \mathbf{0} \\ \mathbf{0} \\ \mathbf{M}_F \\ \mathbf{0} \\ \mathbf{0} \end{bmatrix} \mathbf{E}(t) \begin{bmatrix} \mathbf{0} & \mathbf{N}_F & \mathbf{0} & \mathbf{0} & \mathbf{0} & \mathbf{0} \end{bmatrix} \\
&\leq \underbrace{\begin{bmatrix} \mathbf{0} \\ \mathbf{0} \\ \mathbf{0} \\ \mathbf{M}_F \\ \mathbf{0} \\ \mathbf{0} \end{bmatrix} \varepsilon_6 \begin{bmatrix} \mathbf{0} & \mathbf{0} & \mathbf{0} & \mathbf{M}_F^T & \mathbf{0} & \mathbf{0} \end{bmatrix}}_{LMI} + \underbrace{\begin{bmatrix} \mathbf{0} \\ \mathbf{N}_F^T \\ \mathbf{0} \\ \mathbf{0} \\ \mathbf{0} \\ \mathbf{0} \end{bmatrix} \varepsilon_6^{-1} \begin{bmatrix} \mathbf{0} & \mathbf{N}_F & \mathbf{0} & \mathbf{0} & \mathbf{0} & \mathbf{0} \end{bmatrix}}_{\Omega_6}
\end{aligned} \tag{A5}
$$

$$
\begin{aligned}
\Xi_7 &= \begin{bmatrix} \mathbf{0} & \mathbf{0} & \mathbf{0} & \mathbf{0} & \mathbf{X}\Delta\mathbf{C}_1(t)^T & \mathbf{0} \\ \mathbf{0} & \mathbf{0} & \mathbf{0} & \mathbf{0} & \mathbf{0} & \mathbf{0} \\ \mathbf{0} & \mathbf{0} & \mathbf{0} & \mathbf{0} & \mathbf{0} & \mathbf{0} \\ \mathbf{0} & \mathbf{0} & \mathbf{0} & \mathbf{0} & \mathbf{0} & \mathbf{0} \\ \Delta\mathbf{C}_1(t)\mathbf{X} & \mathbf{0} & \mathbf{0} & \mathbf{0} & \mathbf{0} & \mathbf{0} \\ \mathbf{0} & \mathbf{0} & \mathbf{0} & \mathbf{0} & \mathbf{0} & \mathbf{0} \end{bmatrix} = \begin{bmatrix} \mathbf{X}\mathbf{N}_{c_1}^T \\ \mathbf{0} \\ \mathbf{0} \\ \mathbf{0} \\ \mathbf{0} \\ \mathbf{0} \end{bmatrix} \mathbf{E}(t) \begin{bmatrix} \mathbf{0} & \mathbf{0} & \mathbf{0} & \mathbf{0} & \mathbf{M}_{c_1}^T & \mathbf{0} \end{bmatrix} + \begin{bmatrix} \mathbf{0} \\ \mathbf{0} \\ \mathbf{0} \\ \mathbf{0} \\ \mathbf{M}_{c_1} \\ \mathbf{0} \end{bmatrix} \mathbf{E}(t) \begin{bmatrix} \mathbf{N}_{c_1}\mathbf{X} & \mathbf{0} & \mathbf{0} & \mathbf{0} & \mathbf{0} & \mathbf{0} \end{bmatrix} \\
&\leq \underbrace{\begin{bmatrix} \mathbf{0} \\ \mathbf{0} \\ \mathbf{0} \\ \mathbf{0} \\ \mathbf{M}_{c_1} \\ \mathbf{0} \end{bmatrix} \varepsilon_7 \begin{bmatrix} \mathbf{0} & \mathbf{0} & \mathbf{0} & \mathbf{0} & \mathbf{M}_{c_1}^T & \mathbf{0} \end{bmatrix}}_{LMI} + \underbrace{\begin{bmatrix} \mathbf{X}\mathbf{N}_{c_1}^T \\ \mathbf{0} \\ \mathbf{0} \\ \mathbf{0} \\ \mathbf{0} \\ \mathbf{0} \end{bmatrix} \varepsilon_7^{-1} \begin{bmatrix} \mathbf{N}_{c_1}\mathbf{X} & \mathbf{0} & \mathbf{0} & \mathbf{0} & \mathbf{0} & \mathbf{0} \end{bmatrix}}_{\Omega_7}
\end{aligned} \tag{A6}
$$

$$
\begin{aligned}
\Xi_8 &= \begin{bmatrix} \mathbf{0} & \mathbf{0} & \mathbf{0} & \mathbf{0} & \mathbf{Y}^T\Delta\mathbf{D}_{12}(t)^T & \mathbf{0} \\ \mathbf{0} & \mathbf{0} & \mathbf{0} & \mathbf{0} & \mathbf{0} & \mathbf{0} \\ \mathbf{0} & \mathbf{0} & \mathbf{0} & \mathbf{0} & \mathbf{0} & \mathbf{0} \\ \mathbf{0} & \mathbf{0} & \mathbf{0} & \mathbf{0} & \mathbf{0} & \mathbf{0} \\ \Delta\mathbf{D}_{12}(t)\mathbf{Y} & \mathbf{0} & \mathbf{0} & \mathbf{0} & \mathbf{0} & \mathbf{0} \\ \mathbf{0} & \mathbf{0} & \mathbf{0} & \mathbf{0} & \mathbf{0} & \mathbf{0} \end{bmatrix} = \begin{bmatrix} \mathbf{Y}^T\mathbf{N}_{D_{12}}^T \\ \mathbf{0} \\ \mathbf{0} \\ \mathbf{0} \\ \mathbf{0} \\ \mathbf{0} \end{bmatrix} \mathbf{E}(t) \begin{bmatrix} \mathbf{0} & \mathbf{0} & \mathbf{0} & \mathbf{0} & \mathbf{M}_{D_{12}}^T & \mathbf{0} \end{bmatrix} + \begin{bmatrix} \mathbf{0} \\ \mathbf{0} \\ \mathbf{0} \\ \mathbf{0} \\ \mathbf{M}_{D_{12}} \\ \mathbf{0} \end{bmatrix} \mathbf{E}(t) \begin{bmatrix} \mathbf{N}_{D_{12}}\mathbf{Y} & \mathbf{0} & \mathbf{0} & \mathbf{0} & \mathbf{0} & \mathbf{0} \end{bmatrix} \\
&\leq \underbrace{\begin{bmatrix} \mathbf{0} \\ \mathbf{0} \\ \mathbf{0} \\ \mathbf{0} \\ \mathbf{M}_{D_{12}} \\ \mathbf{0} \end{bmatrix} \varepsilon_8 \begin{bmatrix} \mathbf{0} & \mathbf{0} & \mathbf{0} & \mathbf{0} & \mathbf{M}_{D_{12}}^T & \mathbf{0} \end{bmatrix}}_{LMI} + \underbrace{\begin{bmatrix} \mathbf{Y}^T\mathbf{N}_{D_{12}}^T \\ \mathbf{0} \\ \mathbf{0} \\ \mathbf{0} \\ \mathbf{0} \\ \mathbf{0} \end{bmatrix} \varepsilon_8^{-1} \begin{bmatrix} \mathbf{N}_{D_{12}}\mathbf{Y} & \mathbf{0} & \mathbf{0} & \mathbf{0} & \mathbf{0} & \mathbf{0} \end{bmatrix}}_{\Omega_8}
\end{aligned} \tag{A7}
$$

$$
\begin{aligned}
\Xi_9 &= \begin{bmatrix} \mathbf{0} & \mathbf{0} & \mathbf{0} & \mathbf{0} & \mathbf{0} & \mathbf{0} \\ \mathbf{0} & \mathbf{0} & \mathbf{0} & \mathbf{0} & \mathbf{0} & \Delta\mathbf{F}(t)^T \\ \mathbf{0} & \mathbf{0} & \mathbf{0} & \mathbf{0} & \mathbf{0} & \mathbf{0} \\ \mathbf{0} & \mathbf{0} & \mathbf{0} & \mathbf{0} & \mathbf{0} & \mathbf{0} \\ \mathbf{0} & \mathbf{0} & \mathbf{0} & \mathbf{0} & \mathbf{0} & \mathbf{0} \\ \mathbf{0} & \Delta\mathbf{F}(t) & \mathbf{0} & \mathbf{0} & \mathbf{0} & \mathbf{0} \end{bmatrix} = \begin{bmatrix} \mathbf{0} \\ \mathbf{N}_F^T \\ \mathbf{0} \\ \mathbf{0} \\ \mathbf{0} \\ \mathbf{0} \end{bmatrix} \mathbf{E}(t) \begin{bmatrix} \mathbf{0} & \mathbf{0} & \mathbf{0} & \mathbf{0} & \mathbf{0} & \mathbf{M}_F^T \end{bmatrix} + \begin{bmatrix} \mathbf{0} \\ \mathbf{0} \\ \mathbf{0} \\ \mathbf{0} \\ \mathbf{0} \\ \mathbf{M}_F \end{bmatrix} \mathbf{E}(t) \begin{bmatrix} \mathbf{0} & \mathbf{N}_F & \mathbf{0} & \mathbf{0} & \mathbf{0} & \mathbf{0} \end{bmatrix} \\
&\leq \underbrace{\begin{bmatrix} \mathbf{0} \\ \mathbf{0} \\ \mathbf{0} \\ \mathbf{0} \\ \mathbf{0} \\ \mathbf{M}_F \end{bmatrix} \varepsilon_9 \begin{bmatrix} \mathbf{0} & \mathbf{0} & \mathbf{0} & \mathbf{0} & \mathbf{0} & \mathbf{M}_F^T \end{bmatrix}}_{LMI} + \underbrace{\begin{bmatrix} \mathbf{0} \\ \mathbf{N}_F^T \\ \mathbf{0} \\ \mathbf{0} \\ \mathbf{0} \\ \mathbf{0} \end{bmatrix} \varepsilon_9^{-1} \begin{bmatrix} \mathbf{0} & \mathbf{N}_F & \mathbf{0} & \mathbf{0} & \mathbf{0} & \mathbf{0} \end{bmatrix}}_{\Omega_9}
\end{aligned} \tag{A8}
$$

References

1. Liu, H.; Gao, H.; Li, P. *Handbook of Vehicle Suspension Control Systems*; Institution of Engineering and Technology: London, UK, 2013.
2. Karim Afshar, K.; Javadi, A.; Jahed-Motlagh, M.R. Robust H_∞ control of an active suspension system with actuator time delay by predictor feedback. *IET Control. Theory Appl.* **2018**, *12*, 1012–1023. [CrossRef]

3. Konieczny, J.; Rączka, W.; Sibielak, M.; Kowal, J. Energy consumption of an active vehicle suspension with an optimal controller in the presence of sinusoidal excitations. *Shock Vib.* **2020**, *2020*, 6414352. [CrossRef]
4. Chen, M.; Hu, Y. *Inerter and Its Application in Vibration Control Systems*; Springer: Singapore, 2019.
5. Brzeski, P.; Pavlovskaia, E.; Kapitaniak, T.; Perlikowski, P. The application of inerter in tuned mass absorber. *Int. J. Non Linear Mech.* **2015**, *70*, 20–29. [CrossRef]
6. Brzeski, P.; Kapitaniak, T.; Perlikowski, P. Novel type of tuned mass damper with inerter which enables changes of inertance. *J. Sound Vib.* **2015**, *349*, 56–66. [CrossRef]
7. Wang, Y.; Jin, X.Y.; Zhang, Y.S.; Ding, H.; Chen, L.Q. Dynamic performance and stability analysis of an active inerter-based suspension with time-delayed acceleration feedback control. *Bull. Pol. Acad. Sci. Tech. Sci.* **2022**, *70*, e140687. [CrossRef]
8. Scheibe, F.; Smith, M.C. Analytical solutions for optimal ride comfort and tyre grip for passive vehicle suspensions. *Veh. Syst. Dyn.* **2009**, *47*, 1229–1252. [CrossRef]
9. Hu, Y.; Chen, M.Z.; Shu, Z. Passive vehicle suspensions employing inerters with multiple performance requirements. *J. Sound Vib.* **2014**, *333*, 2212–2225. [CrossRef]
10. Wang, F.C.; Su, W.J. Impact of inerter nonlinearities on vehicle suspension control. *Veh. Syst. Dyn.* **2008**, *46*, 575–595. [CrossRef]
11. Wang, F.C.; Chan, H.A. Vehicle suspensions with a mechatronic network strut. *Veh. Syst. Dyn.* **2011**, *49*, 811–830. [CrossRef]
12. Zhang, X.L.; Liu, J.J.; Nie, J.M.; Chen, L. Design principle and method of a passive hybrid damping suspension system. *Appl. Mech. Mater.* **2014**, *635–637*, 1232–1240. [CrossRef]
13. Sun, W.; Pan, H.; Zhang, Y.; Gao, H. Multi-objective control for uncertain nonlinear active suspension systems. *Mechatronics* **2014**, *24*, 318–327. [CrossRef]
14. Hu, Y.; Du, H.; Chen, M.Z. An inerter-based electromagnetic device and its application in vehicle suspensions. In Proceedings of the 2015 34th Chinese Control Conference (CCC), Hangzhou, China, 28–30 July 2015; pp. 2060–2065.
15. Liu, Y.J.; Chen, H. Adaptive sliding mode control for uncertain active suspension systems with prescribed performance. *IEEE Trans. Syst. Man, Cybern. Syst.* **2020**, *51*, 6414–6422. [CrossRef]
16. Konieczny, J.; Sibielak, M.; Raczka, W. Active Vehicle Suspension with Anti-Roll System Based on Advanced Sliding Mode Controller. *Energies* **2020**, *13*, 5560. [CrossRef]
17. Taghavifar, H.; Mardani, A.; Hu, C.; Qin, Y. Adaptive Robust Nonlinear Active Suspension Control Using an Observer-Based Modified Sliding Mode Interval Type-2 Fuzzy Neural Network. *IEEE Trans. Intell. Veh.* **2020**, *5*, 53–62. [CrossRef]
18. Canale, M.; Milanese, M.; Novara, C. Semi-Active Suspension Control Using "Fast" Model-Predictive Techniques. *IEEE Trans. Control. Syst. Technol.* **2006**, *14*, 1034–1046. [CrossRef]
19. Akbari, A.; Geravand, M.; Lohmann, B. Output feedback constrained H_∞ control of active vehicle suspensions. In Proceedings of the 2010 2nd International Conference on Advanced Computer Control, Shenyang, China, 27–29 March 2010; Volume 3, pp. 399–404.
20. Gao, H.; Sun, W.; Shi, P. Robust sampled-data H_∞ control for vehicle active suspension systems. *IEEE Trans. Control. Syst. Technol.* **2009**, *18*, 238–245. [CrossRef]
21. Chatavi, M.; Vu, M.T.; Mobayen, S.; Fekih, A. H_∞ Robust LMI-Based Nonlinear State Feedback Controller of Uncertain Nonlinear Systems with External Disturbances. *Mathematics* **2022**, *10*, 3518. [CrossRef]
22. Badri, P.; Amini, A.; Sojoodi, M. Robust fixed-order dynamic output feedback controller design for nonlinear uncertain suspension system. *Mech. Syst. Signal Process.* **2016**, *80*, 137–151. [CrossRef]
23. Li, P.; Lam, J.; Cheung, K.C. Control of vehicle suspension using an adaptive inerter. *Proc. Inst. Mech. Eng. Part D J. Automob. Eng.* **2015**, *229*, 1934–1943. [CrossRef]
24. Yu, J.; Yang, C.; Tang, X.; Wang, P. H_∞ control for uncertain linear system over networks with Bernoulli data dropout and actuator saturation. *ISA Trans.* **2018**, *74*, 1–13. [CrossRef]
25. Xia, X.; Hashemi, E.; Xiong, L.; Khajepour, A. Autonomous Vehicle Kinematics and Dynamics Synthesis for Sideslip Angle Estimation Based on Consensus Kalman Filter. *IEEE Trans. Control. Syst. Technol.* **2023**, *31*, 179–192. [CrossRef]
26. Wang, Y.; Xie, L.; De Souza, C.E. Robust control of a class of uncertain nonlinear systems. *Syst. Control Lett.* **1992**, *19*, 139–149. [CrossRef]
27. Zhang, F. *The Schur Complement and Its Applications*; Springer Science & Business Media: Berlin/Heidelberg, Germany; New York, NY, USA, 2006; Volume 4.
28. Lofberg, J. YALMIP: A toolbox for modeling and optimization in MATLAB. In Proceedings of the 2004 IEEE International Conference on Robotics and Automation (IEEE Cat. No.04CH37508), Taipei, Taiwan, 2–4 September 2004; pp. 284–289. [CrossRef]